The interaction profile between CDC20 and the components of the anaphase promoting complex or cyclosome (APC/C) in human Hela cells

2019

Yu Liu
Student Number: 109236410
Supervisor: Dr Jun-Yong Huang
Institute for Cell and Molecular Bioscience
Word count: 12582

Abstract

The mis-segregation of chromosomes during mitosis can lead to genetic disorders, like Down syndrome, birth defects and even cancers (5-9). The spindle assembly checkpoint (SAC) is the most important mechanism in mitosis (3, 10). The SAC functions to prevent premature sister-chromatid segregation - at anaphase onset by inhibiting the premature activation of the anaphase promoting complex/cyclosome (APC/C) by its coactivator CDC20 (cell division cycle protein 20) (10, 12). The APC/C is a large multi-subunit protein complex which functions as an E3 ubiquitin ligase and targets substrates by ubiquitination and consequently destruction by the proteasome throughout the cell cycle (reviewed in 61). It contains three functional subdomains: the scaffolding platform consists of APC1, APC4, and APC5; the catalytic domain consists of APC2 (a Cullin family related protein), APC10 (Doc1) and APC11 (RING finger protein); and the TPR (tetratricopeptide repeat) lobe domain consists of APC3, APC6, APC7, APC8, APC13, APC16 and Cdc26 (Reviewed in 63). The spatiotemporal activation of the APC/C is primarily achieved by sequential and regulated binding to its two co-activators, CDC20 and Cdh1 leading to the formation of APC/C^{CDC20} and APC/C^{Cdh1} which are two E3 ligase complexes (Reviewed in 61). The APC/C^{CDC20} primarily controls the metaphase/anaphase transition and mitotic exit by targeting and destroying Cyclin B1 and securin through regulation by the SAC (Reviewed in 61). More recently, it has been shown that the APC/C can interact with a second CDC20 and target other substrates, such as Nek2A and Cyclin A which are degraded in prometaphase independently of the SAC (64). As the interaction between CDC20 and the APC/C, or the $CDC20^{MCC}$ and the APC/C has never been seen in vivo, it will be important to understand the timing of these interactions and the part that they play in regulating the APC/C (50, 52). Therefore, the overall aim of this project is using PLA to investigate the protein-protein interactions between the components of the APC/C and its co-activator, CDC20; and the interactions among the subunits of the APC/C to provide insights into the regulation of the APC/C. We have studied the in vivo protein-protein interactions between APC3-CDC20, APC8-CDC20, and APC11-CDC20 and intended to examine the interactions between CDC20 and the APC/C. We have also examined the dynamic assembly of the APC/C by looking at APC3-APC6, and APC3-APC10 complexes. Our results suggest that APC11-$CDC20^{APC8}$, and APC11-$CDC20^{APC3}$ interacted at the same time, and we favour the interpretation that there is only one APC/C.

The interaction profiles of the APC3-APC6 and APC3-APC10 suggest that the assembly of the APC/C is cell cycle regulated.

Acknowledgments

I would like to thank Dr Jun-Yong Huang for his dedicated support, patience, and instruction throughout the course of this project. I would also like to thank Fiona Fenwick for her invaluable support in the cell culture lab, and Dr Diana Papini for the gift of the Hela cell.

Table of Contents

1. Introduction

Eukaryotic cells require accurate chromosome segregation for their normal division and stable inheritance. Mis-segregation of chromosome during mitosis will produce daughter cells which are not genetically identical, this can be lethal to the cell or can lead to aneuploidy (9, 10). If it occurs in reproductive cells, aneuploidy can lead to genetic disorders, such as Down syndrome (7, 10, 11). If it occurs in somatic cells, aneuploidy is recognized as a hallmark of cancer (1-5). Cells have therefore evolved a mechanism for monitoring the segregation of sister-chromatids and correcting errors both in mitosis and meiosis, called the spindle assembly checkpoint (SAC) (6, 7). This project predominantly focuses on the SAC in somatic cell division (i.e., mitosis).

Currently, it is believed that during mitosis, the SAC remains active until each pair of sister-chromatids have attached to microtubules through their kinetochores, and appropriate tension has been generated (12). The SAC functions to delay the sister-chromatid segregation - and thus the anaphase onset - by inhibiting the anaphase promoting complex/ or cyclosome (APC/C), through altering the contact between the APC/C and its coactivator CDC20 (cell division cycle protein 20) (6, 8). When all kinetochores on each pair of sister-chromatids have attached to microtubules, and tension has been generated, the SAC is satisfied and CDC20 is freed to activate the APC/C by recognizing and degrading the main mitotic regulator proteins, cyclin B1 and securin, thus facilitating the metaphase to anaphase transition.

Cyclin B1 which activates CDK1 (cyclin-dependent kinase 1) in early mitosis is essential for driving cells to enter mitosis (13-15). Securin locks the cohesin ring complex which holds the sister chromatids together and prevents them from premature segregation (16, 17). By degrading Cyclin B1 and Securin at the end of mitosis, CDK1 kinase activity becomes inactivated and separase is activated to unlock the cohesin ring, releasing the sister-chromatids, an facilitating the metaphase to anaphase transition and mitotic exit. However, Cyclin B1 and Securin are not the sole substrates of the APC/C^{CDC20}, other proteins such as Cyclin A and Nek2A in prophase are also its substrates (18). Moreover, in late mitosis, the APC/C will be activated by another activator, CDC20-homologue 1 (CDH1) (19),

the APC/C^{CDH1} targets more substrates, including Aurora A and UBCH10, etc (18, 20), although CDH1 is not essential for some species (21).

The APC/C has been shown to function from mitosis to late G1 (growing phase 1) (19, 22), and its substrate specificity is partly regulated by its co-activators, CDC20 and CDH1 (23). In *Drosophila*, it has been shown that CDC27 (APC3) and CDC16 (APC6), the core components of the APC/C, are differentially localised to mitotic chromosomes and spindle microtubules, which suggests that multiple forms of the APC/C might exist (64). More recently, it has been suggested that by interacting with different component of the APC/C, for instance APC3 and APC8 in prophase and metaphase, CDC20 can mark different substrates such as cyclin A and cyclin B1 for ubiquitination and hence degradation (20). However, exactly when and where the interactions between CDC20 and these APC/C subunits occurs in vivo has never been discovered. Also, if the formation of the multi-subunit complex of the APC/C is cell cycle regulated or if it persists throughout the cell cycle were remains unknown. In this project, we have investigated these issues by studying the interactions between some of the APC/C subunits and CDC20 based on single cell analysis using the Duolink-mediated proximity ligation assay (The technical details of the assay will be discussed later).

1.1 The Eukaryotic Cell Cycle

The growth and survival of all eukaryotic organisms relies on mitotic cell division, by which two genetically identical daughter cells are produced from one original mother cell, which allows the organism to grow, metabolise and repair its damaged tissues (24). The eukaryotic cell cycle is normally comprised of four stages: growth phase 1 (G1), synthesis phase (S), growth phase 2 (G2) and mitosis (M). In G1, cells increase their size. Once they have grown to their proper size, cells then enter S phase, where DNA duplication occurs. After S phase, cells continue to grow during G2, and accumulate essential resources, such as amino acids. M phase is the final stage of the cycle, during which the cell divides and separates into two identical daughter cells, each of which will then undergo their own next round of the cell cycle. Some cells can exit the cell cycle by entering a quiescent state called G0 at late G1. Cells in G0 such as neurons remain quiescent. G1, together with the S and G2

phases are collectively known as 'interphase': the period between mitotic divisions (shown in Figure 1)

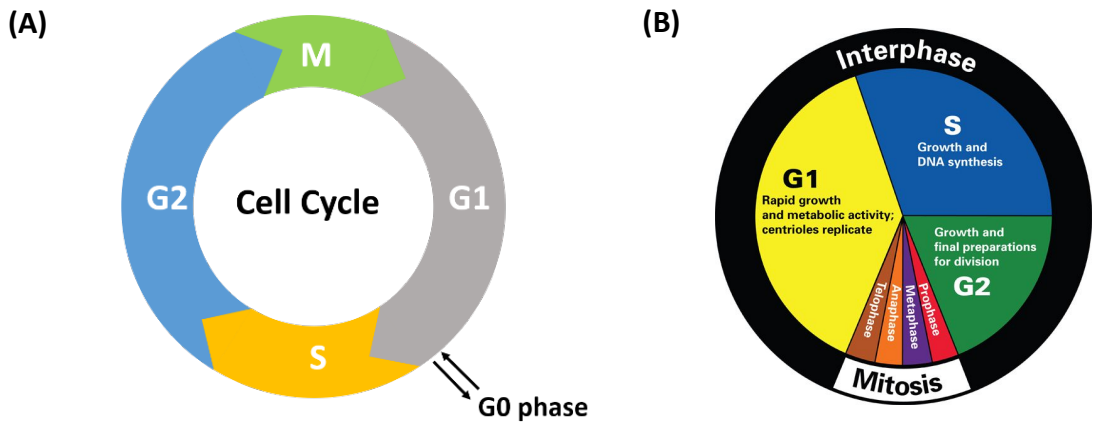

Figure 1. The partition of the main eukaryotic cell cycle stages

Schematic diagram shows a typical eukaryotic cell cycle. An entire cycle is divided into four parts. The four parts represent the four stages: mitosis (M), growth phase 1 (G1), synthesis phase (S) and growth phase 2 (G2). Some types of cell have G0 phase within G1 (A). The interphase constitutes phases G1, S and G2, the rest of cell cycle is mitosis (B).

Mitosis itself can then be subdivided into distinct stages: prophase, prometaphase, metaphase, anaphase and telophase.

In prophase, the duplicated DNA begin to condense to form sister-chromatids, and after the nuclear envelope has broken down (NEBD) marking the end of prophase, cells then enter prometaphase. Kinetochores are formed at the centromere region of the sister chromatids, microtubules are nucleated from both the centrosomes and the centromeres, and these microtubules begin to search for and interact with unattached kinetochores (25, 26). The proper attachment of kinetochores induces changes both on kinetochore conformation and mitotic spindle dynamics, which in turn generates the pulling force that drives the chromatid towards the plus end of the spindle. Spontaneously, the counteracting force is produced by the SAC to maintain the temporal geometry of the sister chromatids (25, 26, reviewed in 83, 84). Once all of the kinetochores have been properly bound by microtubules, the SAC is satisfied and the counteracting force is eliminated allowing each pair of chromosomes to be pulled apart, and allowing anaphase to be initiated (27-29). During anaphase, the sister chromatids are separated and pulled to the spindle poles. As mentioned above, the separation of sister chromatids requires the breakdown of the

cohesin ring complex (16, 17). Finally, the destruction of cyclin B to inactivate the CDK1 kinase activity will allow the chromatids to decondense and the daughter nuclear envelope membranes to reform in telophase, and then during cytokinesis, two daughter cells are formed (24). These processes are illustrated in Figure 2.

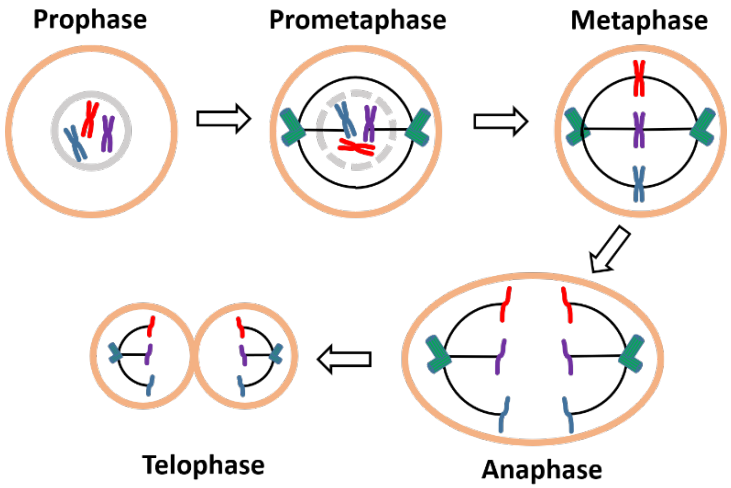

Figure 2. Mitotic sub-stages

Schematic diagram shows the five substages of mitosis. The Orange circles represent cells, the grey circle in solid and dashed lines are the nuclear envelop and broken nuclear envelop, respectively, the green tickles are centrosomes, the dark green lines are microtubules and the red and blue lines are different pairs of sister-chromatids.

Here the question raised is, how do the cell cycle stage, as well as the mitotic substages progress in a sequential manner? Cell cycle progression is driven by cyclin dependent kinases (CDKs) and their cyclin partners (30). Once bound to their corresponding cyclins, CDKs are activated, and acquire the ability to phosphorylate their substrates which switches on their activity and drives the cell to enter the next stage. Since the expression of the CDKs is constant throughout the cell cycle, it is the up- and down-regulation of the cyclins that is key to controlling such events. Each CDK has fixed cyclin partner(s) and each combination functions at a specific stage (30), (Figure 3).

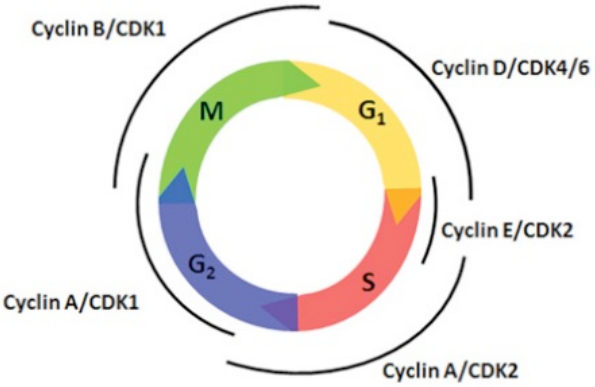

Figure 3. Cyclin-CDK regulation of the cell cycle

Adapted from Reference (30). In mammalian cells, the progression of the cell cycle is regulated by different cyclin-CDK complexes through at different stages.

As mentioned above, CDK1 activity is crucial for the cell remaining in a mitotic state, and the progression of mitosis is dependent on cyclin B-CDK1 (31, 32). At the same time, although Cyclin B is ubiquitylated by the APC/C and subsequently marked for degradation, the APC/C itself is also a substrate of Cyclin B-CDK1 (33). In early mitosis, the activation of the APC/C is a binary process through Cyclin B-CDK1 phosphorylation. Firstly, the phosphorylation of the APC/C core subunits (e.g., APC7, APC3, APC6 and APC8) facilitates the binding of CDC20 (30, 34, 35); secondly, the phosphorylation of CDH1 prevents it from binding to the APC/C; and thus ensures that APC/C-CDC20 is the sole ubiquitin ligase at this stage (36). Once activated, the APC/C-CDC20 complex initiates the ubiquitination and degradation of cyclin B (13-15). In late mitosis, the declining level of cyclin B results in cyclin B-CDK1 inactivation, which in turn stops the phosphorylation of CDH1. CDH1 then binds to the APC/C, and the APC/C-CDH1 complex targets CDC20 as one of its substrates, and therefore facilitates the cell to enter the G1 phase (13, 37-40). In conclusion, the interplay of the APC/C and cyclinB-CDK1 controls the progression and exit of mitosis through a process of feedback regulation.

1.2 The Spindle Assembly Checkpoint

Cell cycle progression requires tight control. Like a car moving along a road, the cell cycle requires not only the accurate timing of various CDK activities to drive it forward, but also regular checks to rule out malfunctions along the way. In cells, such 'checks' that ensure proper cell cycle progression are called cell cycle checkpoints. There are three main

checkpoints throughout the cycle: the G1 checkpoint, the G2/M checkpoint, and the metaphase-anaphase checkpoint (40).

The G1 phase is the time between the end of mitosis and the beginning of DNA replication in S phase. The G1 checkpoint, is also known as the restriction point in mammalian cells and the start point in yeast, it is the point where the cell decides to either re-enter a cell cycle or to enter a quiescent state known as G0. The checkpoint delays the G1 phase in response to the cell size, nutrients, growth factors, or DNA damage (41). The G2/M checkpoint is a DNA damage checkpoint, which detects DNA damage, such as base loss, single-strand breaks or double-strand breaks. Once damage is detected, this checkpoint activates repair systems to fix them, or it will induce programmed cell death if the amount of damage is beyond repair. Therefore, the integrity and health of the genetic material is guaranteed for the following division (42, 43).

The checkpoint involved at the metaphase-anaphase transition is the spindle assembly checkpoint (SAC), which delays anaphase onset to guarantee accuracy of chromosome segregation (6). The SAC is believed to be activated after NEBD, and lasts until the last kinetochore - microtubule attachment is completed properly (7). Some people believed that satisfaction of the SAC requires both attachment to and tension on the kinetochore (11, 27, 28, 44), whereas more recent papers suggest that the tension is more likely to be an attribute of proper attachment, which is created by the antagonistic forces between spindle dynamics and SAC protein maintenance (84, 86). A lack of tension is largely due to unstable binding, which activates a pathway that leads to the phosphorylation of the Aurora B kinase substrate for error correction (87). Therefore, tension appears to be an essential index of robust MT-KT interaction, rather than a prerequisite for satisfaction of the SAC (87, 88). The kinetochore is the origin of the signal for activating the SAC, and the SAC strength varies according to the amount of unattached kinetochore (29, 43). The SAC pathway behaves as a cascade, and the assembly of the kinetochore is a prerequisite for recruiting SAC proteins. In mammalian cells, the centromeric DNA associates with centromeric protein A (CENP-A), a histone 3 variant, which provides a docking site for recruiting 16 centromere proteins (CENPs) to assemble as constitutive centromere network (CCAN), which forms inner kinetochore (29). The inner kinetochore recruits the 'KMN network' as the outer kinetochore just before NEBD. The KMN network is a protein complex

composed of kinetochore null protein 1(KNL1, also known as Blinkin), the mis-segregation 12 complex (MIS12) and nuclear division cycle 80 complex (NDC80), which is crucial for microtubule interaction and cascading of the SAC signalling (28, 29, 45). At the unattached kinetochore, a monopolar spindle 1 (MPS1) kinase is tethered to the kinetochore by a phosphorylated Aurora B. This allows MPS1 to phosphorylate KNL1 (46) which subsequently binds BUB1 and BUB3, and recruits BUBR1/Mad3 to form the BUBR1-BUB3 complex, as well as the ROD-ZW10-Zwilch (RZZ) complex, which is a kinetochore receptor for motor dynein-dynactin. These proteins together recruit a MAD1-C-MAD2 heterodimer which can recruit and convert the soluble open form of MAD2 (O-MAD2) into the closed form of MAD2 (C-MAD2) on the kinetochore. This in-turn facilitates the binding of C-MAD2 with CDC20 to form the MAD2-CDC20 complex. The C-MAD2-CDC20 complex binds to the BUBR1-BUB3 complex in an as yet unknown manner to form the mitotic checkpoint complex (MCC), which is regarded as the core APC/C inhibitor (28) (Figure 4).

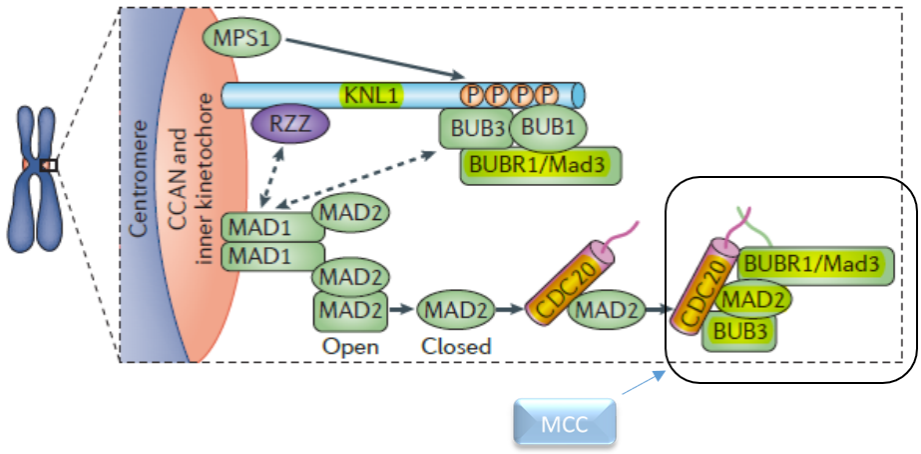

Figure 4. Schematic of the SAC signalling pathway

Adapted from reference (28). The SAC proteins are recruited to the kinetochore in a cascade and eventually form an MCC complex to suppress CDC20.

It used to be believed that the MCC inhibited the APC/C through a binary mechanism. On the one hand, MAD2 directly binds to CDC20 to prevent it from binding and coordinating with the APC/C (47, 48). This in turn, prevents the APC/C complex recognizing and recruiting substrates, which contain the destruction box (D box) motif (18, 20), thereby inhibiting the activation of the APC/C. On the other hand, the BUBR1 of the MCC inhibits the APC/C by preventing substrates from binding to the APC/C, either by inducing a conformational change in the APC/C, or by acting as a 'pseudosubstrate' (10, 49). However, more recently, it

has been suggested that the MCC can inhibit a second CDC20 which has already bound and activated the APC/C (50). The APC/C activated by the second CDC20 can target Cyclin A for degradation in a SAC independent manner, and the APC/$C^{CDC20\text{-}MCC}$ is responsible for the degradation of Cyclin B1 in a SAC dependent manner (52). As the in vivo interaction between the CDC20 and the APC/C, or the $CDC20^{MCC}$ and the APC/C has never been determined, an understanding of the exact timing of these interactions will be important for determining the mechanism of regulating the APC/C.

1.3 The Anaphase Promoting Complex

As previously mentioned, the progression of the cell cycle is modulated by the activity of various CDKs, and the levels of their cyclin partners. These levels are in-turn controlled by the ubiquitin proteasomic system (UPS). The UPS consists of three types of enzymes - termed E1, E2 and E3 - which perform a cascade of reactions, resulting in a post-translational modification named ubiquitylation (50, 51). Firstly, ubiquitin (Ub) is bound and activated by the E1 (ubiquitin-activating enzyme) (18). Then the activated ubiquitin is transferred to the E2 (ubiquitin-conjugating enzyme) (18). The E2 and substrate are brought together by the E3 (ubiquitin-ligase), which contains both an E2 binding site and a substrate binding site. Ubiquitin is then transferred to the substrate to form a polyubiquitin chain at lysine residues (18, 52). Finally, the ubiquitylated protein is degraded by the 26S proteasome (18, 51) (Figure 5).

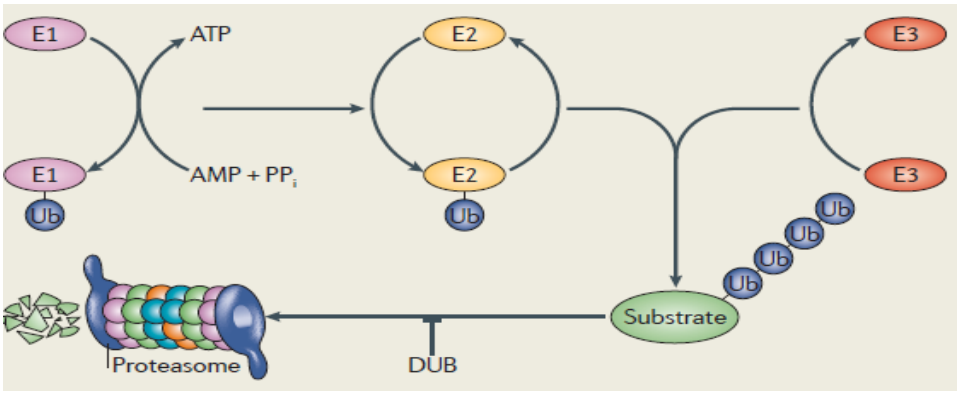

Figure 5. The pathway of ubiquitylation

Adapted from reference (14). Ub represents ubiquitin, PP_i represents inorganic diphosphate, and DUB is deubiquitylating enzyme which can remove the ubiquitin chains from the substrate.

In addition to the cyclins, once the CDK-cyclins complexes are formed, there is a group of proteins that act as negative regulators, called CDK inhibitors (CKIs). The balance between the Cyclins and the CKIs controls the timing of the activity of the CDKs throughout the cell cycle (50). The degradation of the CKIs is also via ubiquitylation (50). Therefore, ubiquitylation is a crucial mechanism involved in controlling cell cycle progression, not only by promoting substrate degradation, but also regulating the stability, localization and even function of the substrate (50, 53). In human cells, there are two E1 enzymes, around 50 E2 enzymes and around 600 E3 enzymes (54). However, the substrate specificity of the target protein depends only on E3 (51). The E3 ligases are divided into 3 classes: cullin-based E3s, HECT-based E3s and RING (really interesting new gene) -finger based E3s (55). Two E3s from the RING-finger based class are involved in regulating the progression of the cell cycle: termed the SKP/cullin/F-box-containing (SCF) complex and the APC/C as mentioned above (51). The two complexes collaborate with each other; their activities covering the whole cell cycle. The SCF complex is activated from late G1 to early M phase, whereas the APC/C functions from the middle of M phase until the end of G1 (50).

The SCF complex contains four subunits. Three of them are conserved (Skp1, Rbx1 and Cullin1) and the other one is a variable F-box-protein which helps bind to specific substrate proteins by recognizing phosphorylated sequences, as shown in Figure 6 (50). The F-box protein Skp2 is the substrate of APC/C^{CDH1}, at the end of G1. With the inactivation of APC/C^{CDH1}, Skp2 is released from its suppression by the APC/C^{CDH1}, and therefore is able to bind and activates the SCF (50, 56). The SCF^{SKP2} complex ubiquitylates CKIs such as p27 and p21, in turn producing the activation of CDK2-Cyclin E, and commencing the onset of S phase (57, 58). The SCF^{SKP2} complex also ubiquitylates Cdt1 and Orc1, which promote the transition from S phase to G2. By the end of G2, another F-box protein, β-Trcp is joining in. $SCF^{\beta\text{-Trcp}}$ drives mitotic progression by targeting Wee1 and Emi1 for degradation. Wee1 inhibits CDK1 and Emi1 is an APC/C inhibitor; thus, both act as mitotic inhibitors (60). Subsequently, after Emi1 is degraded the control of the cell cycle is shifted to the $APC/C^{CDC20\text{-}MCC}$ complex and in early mitosis targets substrates such as Cyclin A and Nek2A in an SAC-independent manner (61), and the APC/CCDC20 is activated at the end of the mitosis targeting Cyclin B and securin (61).

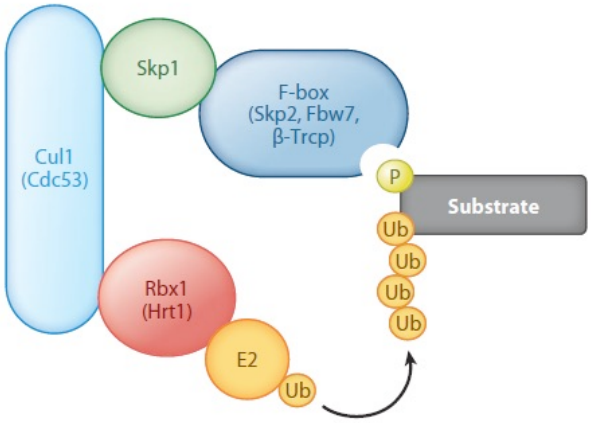

Figure 6. A schematic representation of the SCF complex

The SCF complex is composed of a cullin like protein Cul1 which serves as the scaffold, a RING-finger protein Rbx1 which recruits an E2 enzyme, an adaptor Skp1 which recruits the variable F-box protein. Adapted from reference (53).

The APC/C is a large protein complex composed of at least 13 subunits (depending on the species). Figure 7 shows the schematic of the human APC/C (60).

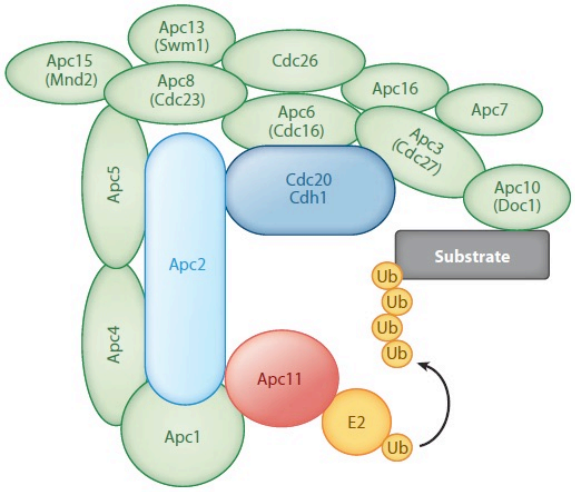

Figure 7. A schematic representation of the human APC/C

The vertebrate APC/C is composed of 14 different subunits and is organised into three structural domains. APC1-APC4-APC5 serves as a scaffolding platform; the cullin-like protein APC2 and a RING-finger protein APC11 serves as the catalytic domain that interacts with E2s; the rest of the TPR proteins forms the TPR domain together with the adaptors CDC20 or CDH1 act as the substrate recognition and recruitment domain. Modified and adapted from ref (53).

The structure of the APC/C is significantly more complicated than that of the SCF complex, although there are corresponding subunits: APC2 substituting for Cul1 and APC11

for Rbx1. Unlike the SCF complex, the APC/C has two alternative coactivators: CDC20 and CDH1. The function of CDC20 is to degrade the mitotic cyclins and securin by recognizing their destruction box (D-box) motif (RXXLXXXXN) before anaphase onset (61). Once the B type cyclins have been degraded, the cyclin B-CDK1 is inactivated allowing CDH1 to be activated by removing its phosphorylation. The active CDH1 binds to the APC/C to form the APC/C-CDH1 complex and CDC20 itself will become a substrate of the complex (61). CDH1 continues to act as the activator of the APC/C by recognizing both the D-box and the KEN box (KENXXXN) motifs from late M phase until the end of the G1 phase (62, 63).

Whilst CDC20 starts to accumulate during S phase the APC/C^{CDC20} is not fully active until the metaphase-anaphase transition (51) and in early mitosis, Emi1 functions as the APC/C inhibitor. Following Emi1 degradation, the SAC is actived and the APC/C is inhibited by the MCC complex. However, even in the presence of an active SAC some substrates such as Nek2A and cyclin A can still be degraded (64-66). Nek2A is a centrosomal kinase that phosphorylates C-Nap and Rootletin which promotes centrosome separation and bipolar spindle formation (66). It has a C-terminal methionine-arginine (MR) tail that binds to the APC/C subunits directly. Cyclin A functions on the initiation of chromosome condensation and probably the NEBD (62, 67, 68). It is still unclear exactly how Nek2A is degraded by the APC/C^{CDC20} (64, 66), but evidence suggests that CDC20 can bind to different sites on the APC/C depending on the state of the SAC. For example, CDC20 requires binding to APC3 and APC8, and the involvement of APC10 when the SAC is satisfied and Cyclin B1 and securin are being degraded; but only requires binding to APC8 to degrade Cyclin A while the SAC is active.

Once the SAC is satisfied, the APC/C^{CDC20} is fully activated and starts to target the main mitotic regulators: cyclin B1 and securin, as shown in Figure 8.

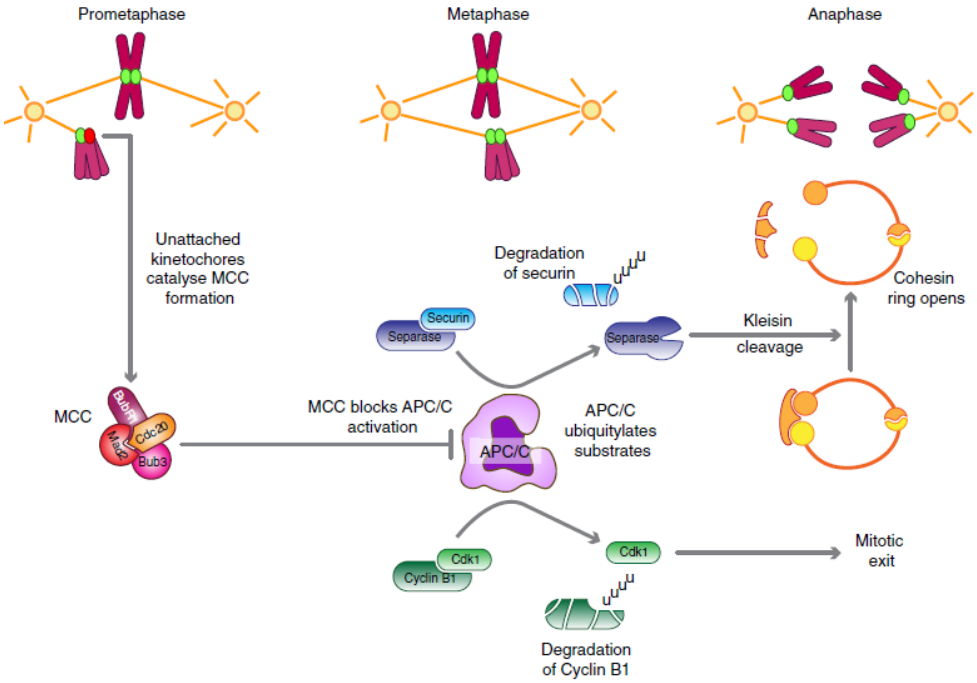

Figure 8. The principles of spindle assembly checkpoints

Adapted from reference (10). Once the APC/C is released from MCC blockage, cyclin B1 is degraded to inactivate CDK1 and securin is degraded to free separase.

As described above when cells enter anaphase, the degradation of cyclin B1 leads to the inactivation of the CDK1-Cyclin B1 complex and in yeast another APC/C coactivator, CDH1, is dephosphorylated by CDC14 and activated (69). The activated APC/C^{CDH1} degrades CDC20, Plk1, Aurora A and Aurora B, in that order (62). However, why there is an ordered destruction for the APC/C^{CDH1} substrates is poorly understood.

The APC/C^{CDH1} continues to function in the G1 phase, targeting CDC6 and geminin maintaining G1, and the initiating DNA replication (18, 70). At the end of G1, CDH1 is inactivated both via inhibitor binding and by phosphorylation by the CDK-cyclins (18). Once CDH1 is inactivated, the F-box protein Skp2 is activated again, and the APC/C gives control of the cell cycle back to the SCF complex (63).

It is understandable that substrate degradation by the APC/C^{CDH1} complex should come after that by the APC/C^{CDC20} complex, as CDH1 can help recognize both the D-box and KEN box motifs. In addition, it has been suggested that binding of CDH1 induces a conformational change in the APC/C, which favours the interaction of APC/C^{CDH1} with its substrates (63, 70). It is, however, quite surprising that there is such a tightly ordered degradation of the substrates by the two coactivators.

At present there is no good explanation as to how the APC/C^{CDC20} can target cyclin A and Nek2A right after M phase onset, but then quickly shift to cyclin B1 and securin once the SAC is satisfied and most hypotheses are centered around the inherent complexity of the APC/C. Theoretically, only four components of the APC/C complex have corresponding subunits in the SCF: the catalytic subunits APC2 and the substrate recognition subunits APC11, and APC10. As a result, research into the control of the timing and specificity of the APC/C activity is focusing on how the other APC/C subunits function.

It has been suggested that specific TPR (tetratricopeptide repeat) protein(s) are required for particular APC/C^{CDC20} substrates (64). APC7, APC3, APC6 and APC8 are four TPR proteins, they are V-shaped dimers, providing binding sites for the scaffolding subunit APC10 and one of the activators, which forms a cavity that is thought to be an interaction site with the substrate (70). However, if this is true, is it necessary that all the APC/C subunits are present all the time? It is proposed that CDC20 and CDH1 bind to different regions of APC3 and APC8 (61). In addition, a *Drosophila melanogaster* study indicates that APC3 and APC6 might have distinct locations before anaphase onset (71). Over the past decade, our understanding of the APC/C has increased dramatically. It has been shown that, as well as regulating cell cycle progression, the APC/C also functions in cell metabolism, cell mobility and gene transcription (61). Nevertheless, how the APC/C is assembled, and whether it requires all its fifteen subunits for every cell cycle stage, and every circumstance, remains unknown; as does how the APC/C collaborates with its activators to change substrate specificity in a sequential manner. In this project, we aim to investigate these unknowns by studying the interaction between certain APC/C subunits and the coactivator CDC20, throughout the cell cycle.

1.4 Proximity Ligation Assay (PLA)

To approach these questions, *in situ* proximity ligation assay (PLA) was the main technique used for visualising and quantifying the protein-protein interactions. The technique was first developed to detect protein-protein interactions between endogenous Myc and Max oncogenic transcription factors in response to interferon-gamma (IFN-gamma) signalling and low-molecular-weight inhibitors in 2006 (83). PLA is one of a few widely used (83, 84). PLA is one of a few widely used and commercially available methods for analyzing protein-protein interactions in their native state (http://www.olink.com/products/duolink/

applications/protein-interactions) (83-85). PLA utilizes two primary antibodies raised in different species to recognize the target antigens of interest, followed by using species specific secondary antibody probes with oligonucleotide conjugated tails to detect the potential interaction if the target proteins are within 40nm distance (71-74). PLA can detect the protein-protein interaction in spatial and temporal profiles within a single cell without the requirement of making fusion proteins. However, there are some weaknesses to the technique that need to be borne in mind. Firstly, the signals detected from two target proteins which are within 40nmof each other does not necessarily represent a true physical interaction. Secondly, the final signal output is polymerase dependent and therefore its sensitivity might vary (76). Furthermore, although PLA can assign signals to specific subcellular locations such as the cytoplasm or the nucleus (83), it might not provide sufficient accuracy to localize the signals to superstructures like the kinetochores. Therefore, in this project, we have not tried to identify any potential kinetochore signals either qualitatively or quantitatively. We have tried to maintain consistent experimental conditions throughout the project and to use appropriate control experiments, such as western blots, APC inhibitory drug treatment, and CO-IP, etc. for comparison and verification.

1.5 Aims

As discussed above that the APC/C activated by a second CDC20 can target Cyclin A for degradation in SAC independent manner, and the $APC/C^{CDC20\text{-}MCC}$ is responsible for the degradation of Cyclin B1 under SAC regulation (52). As the interaction between the CDC20 and the APC/C, or the $CDC20^{MCC}$ and the APC/C has never been revealed in vivo of the cells, it will be important to understand the timing profiles of these interactions for understanding the mechanisms of regulating the APC/C (50,52). Therefore, the overall aim of this project is using PLA to investigate the protein-protein interactions between the components of the APC/C and its co-activators, CDC20; and the interaction profiles among the subunits of the APC/C to provide insights into the regulation mechanisms of the APC/C.

2. Materials and Methods

2.1 Duolink PLA staining

2.1.1 Antibodies

Primary antibodies that were used are listed in Table 1.

Antibodies	Concentration	Type	Manufacturer	Code
Human Anti-BubR1	200µg/ml	Mouse, Polyclonal	Abcam	ab54894
Human Anti-Mad2	200µg/ml	Rabbit, Polyclonal	Thermo	PAS-21594
Human Anti-CDC20	200µg/ml	Mouse, Monoclonal	Santa Cruz	Sc-13162L
Human Anti-APC3	200µg/ml	Rabbit, Polyclonal	Santa Cruz	Sc-5618
Human Anti-APC6	200µg/ml	Rabbit, Polyclonal	Santa Cruz	Sc-5615
Human Anti-APC8	200µg/ml	Rabbit, Polyclonal	Santa Cruz	Sc-20988
Human Anti-APC10	200µg/ml	Rabbit, Polyclonal	Santa Cruz	Sc-20989
Human Anti-APC11	200µg/ml	Goat, Polyclonal	Santa Cruz	Sc-214228
Human Anti-Pericentrin	200µg/ml	Rabbit, Polyclonal	Abcam	Ab4448
Random Immunoglobulin G	N/A	Rabbit	In House	N/A
Random Immunoglobulin G	N/A	Mouse	In House	N/A

Secondary antibodies: The Duolink *in situ* anti-rabbit PLUS, anti-mouse MINUS, anti-goat MINUS was purchased as part of the Duolink PLA kit (distributed by Sigma-Aldrich). For centrosome staining, the secondary antibody used was a goat anti-rabbit Dylight 488 nm antibody (ab96899, Abcam) for pairing with the pericentrin primary antibody.

2.1.2 Buffer preparation

Buffer A: 0.01M Tris (Fisher-Scientific, Loughborough UK), 0.15M sodium chloride (Fisher-Scientific, UK) and 0.05% Tween-20 (Sigma-Aldrich) were prepared using high purity water and the pH was adjusted to 7.4 with appropriate amount of hydrochloric acid (HCl) (Sigma-Aldrich).

Buffer B: 0.2M Tris (Fisher-Scientific, Loughborough UK) and 0.1M sodium chloride (Fisher-Scientific, UK) were prepared using high purity water and the pH was adjusted to 7.5 with appropriate amount of HCl (Sigma-Aldrich).

1XPBS solution: The original PBS (Sigma-Aldrich) solution (10x) was diluted to 1 x PBS in high purity water.

0.2% PBST: Appropriate amount of Tween-20 was prepared in 1X PBS.

Pericentrin antibody blocking solution (homemade): 0.225g glycine was added into 5ml 0.2% PBST, add 1ml goat serum and 2ml 5% BSA, top up with high purity water to 10ml to give the working concentration of 1% BSA, 10% goat serum, 0.3M glycine in 0.1% PBST.

2.1.3 Hela K cell culture

Hela K (Kyoto, named after Kyoto University, Japan) cells were kindly provided by Dr Diana Papini (Newcastle University) as a gift.

DMEM complete Medium for cell culture: 10% (v/v) fetal calf serum (Sigma-Aldrich), 1% glutamine (Sigma-Aldrich), 1% penicillin/streptomycin (Sigma-Aldrich) and 1% nonessential amino-acids (Sigma-Aldrich) were added under a sterilized hood to Dulbecco's Modified Eagle medium (DMEM; Sigma-Aldrich).

Cell culture: HeLa K cells were cultured in 75cm^2 flasks with complete medium at 37℃ and 5% CO_2. The culture media was changed about every 2 days, and the cells were split according to their growth (normally the cells would be split after reaching 70~80% confluence): by removing the media first from the culture flask, followed by washing with 5ml 1xPBS. Then, 3ml trypsin (Sigma-Aldrich) was added, and the flask incubated at 37℃, 5% CO_2 for 3 minutes to detach the cells from the flask. After incubation, 6ml complete DMEM media was added into the flask in order to suspend the trypsin activity. 5ml of this cell culture solution was removed after a proper rinse and agitation (therefore about 5/6 cells were removed) and replaced with 11ml fresh complete media for maintaining the cell culture.

Coverslips preparation: 10 mm diameter round bioscillate glass coverslips (VWR, Leuven, Belgium) were sterilized in 100% ethanol for 5 minutes and left under the hood for air drying. they were then soaked in 100ug/ml Poly-lysine (Sigma-Aldrich) for 5mins, to enhance cell-adherence before being allowed to dry for 2 hours. Each coverslip was placed into one of the 24 wells of a sterilized plate (Santa Cruz) for cell culture.

Cell fixation: After trypsinisation, the cells were harvested from the culture flask and the cell population was counted using a Nexcelom Auto T4 cellometer (Lawrence, MA, USA). The number of cells was adjusted, as required for each individual experiment (normally about 30000 ~ 35000 cells per coverslip in 0.5ml medium), 0.5 ml properly re-suspended cell

solution in medium was split into each well of the plate that held coverslips. Cells were left to grow overnight at 37℃, 5% CO_2. The next day, the medium was removed, and the wells gently washed with 1xPBS; then the cells were fixed with 1ml pre-cooled (–20℃) methanol and kept at -20℃ for use.

2.1.4 Drug treatment

Drugs:

DAME (tosyl-L-arginine methyl ester) was purchased from Santa Cruz. The working concentration used was 25uM in the final medium.

AAME (acetyl-L-arginine methyl ester) was purchased from Calbiochem. The working concentration used was 25uM in the final medium.

APCin (anaphase promoting complex Inhibitor) was purchased from Boston Biotech. The working concentration used was 25uM in the final medium.

DMSO (dimethyl sulfoxide) was purchased from Sigma-Aldrich.

Treatment: The drugs were dissolved into complete medium at a concentration of 25uM. After the cells had been incubating in the 24 wells plate overnight, the medium in the wells was removed, and replaced with the drug containing medium. This was then incubated at 37^{o}C, 5% CO^2 for 24 hours to allow the cells to grow. Photos for each well were taken from three random areas before fixation. The cells were fixed as described above.

2.1.5 Duolink PLA staining procedure

The Duolink PLA assay was used to detect protein-protein interactions or the profile of protein expression in individual cells. In this assay, the primary antibodies are used to target proteins of interest and the specific secondary antibodies are used to recognize the primary antibodies. The oligo tails conjugated on the secondary antibodies are ligated to form a template for rolling circle amplification (RCA) if the two target proteins maintain physical contact or a gap of less than 40nm. An oligonucleotide that is made up of the complementary sequence to the repetitive unit, and conjugated with a specific fluorescent dye, binds to the single-stranded DNA (ssDNA) sequence. This makes the RCA detectable through a fluorescence microscope with the appropriate wavelength. The cell cycle stages can then be determined by the centrosome morphologies (stained by pericentrin) and DNA morphologies (stained by DAPI). Figure 9.

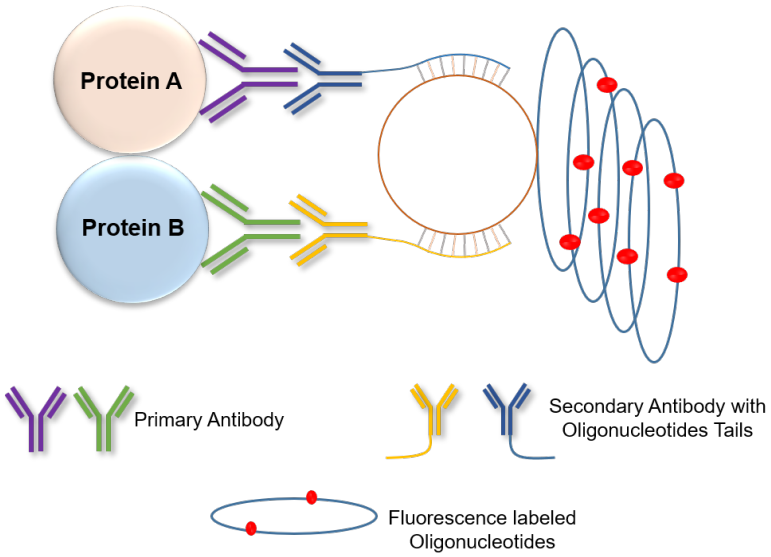

Figure 9. Schematic of the mechanism of the Duolink based proximity ligation assay (PLA)
This PLA uses species-specific primary and secondary antibodies to detect proteins of interest. Secondary antibody probes have oligonucleotide tails. The tails can be ligated together when the two targeted proteins are physically interacting or are less than 40 nm apart. The ligated oligo tails then serve as a template for rolling circle amplification via the polymerase chain reaction, which incorporates fluorescent-tagged oligonucleotide to form the fluorescent signal product. The fluorescence is measured by confocal microscopy.

We used the following Duolink PLA staining protocol for this study:

Blocking non-specific binding: After appropriate fixation, each coverslip was transferred from the 24-well plate into the well of 12-well assay culture plate (Santa Cruz), on a pre-placed parafilm disc. Cells were rehydrated and permeabilized with 0.2% PBST for 6mins, and washed twice with 1xPBS for 5mins followed by blocking with 25µl pericentrin blocking solution at room temperature for 15 minutes.

Primary antibody incubation: 20µl of 1:200 diluted primary antibody (raised in mouse and rabbit, respectively) in PLA diluent was loaded onto each coverslip, after removal of the pericentrin blocking solution using a strip of whatman paper (GE Lifesciences, Little Chalfont, UK). They were then incubated at 37°C for 120 minutes or overnight at 4°C.

Secondary antibody incubation: After washing with 1xPBS, 15µl commercial secondary antibody dissolved in PLA diluents (with 1:500 dilution) was loaded onto the coverslips and incubated at 37°C for 1 hour.

Ligation reaction: The secondary probed coverslips were then washed with Buffer A (2x5 minutes with gentle agitation), 15µl of the ligation solution was then added (2% ligase, 18% ligation stock, 80% purified water), followed by Incubation at 37°C for 30 minutes.

Amplification reaction: After washing with buffer A (2x2 minutes with gentle agitation), 15µl amplification solution (1% polymerase, 19% amplification stock, 80% purified water) was added, followed by incubation at 37℃ for 120 minutes.

Centrosome staining with pericentrin primary antibody: After washing with buffer B (2x5 minutes), 20µl primary pericentrin antibody (diluted in PLA diluent at a dilution factor of 1:500) was added onto each coverslip, followed by incubation at room temperature for 1.5 hours.

Centrosome staining with pericentrin secondary antibody: After washing with 1x PBS (2x5 minutes), 20µl goat Anti-rabbit Dylight 488nm antibody (1:500 dilution) was added to each coverslip, followed by incubation at room temperature for 1 hour.

DNA staining with DAPI: After washing with 1x PBS for two times, 15µl DAPI (1:3000 diluted in PBS) was added to each coverslip, followed by incubation at room temperature for 15 minutes.

Mounting coverslips: After washing with 1 x PBS solution (2 x 5 minutes), the coverslips were air dried on blue roll paper, mounted on microscope slides (Academy Science, Beckenham, UK) with 5µl mounting solution and sealed with nail glue.

Imaging acquisition using confocal microscope system: Samples were scanned using a Leica SP2 confocal laser scanning microscope system with 'HCX APO CS' 40 x 1.25 oil objective lens. The laser excitation wavelengths were set at 405nm for detecting DAPI, 488nm for the FITC (fluorescein isothiocyanate) signal and 594nm for the TexasRed (sulforhodamine 101 acid chloride) fluorescence produced by the proteins of complexes of interest. The laser powers were set at 34% throughout the scanning for all experiments.

Quantification for fluorescent signals: Z-stack section images were projected to produce a single image for quantification of the collective maximum fluorescence intensity to represent the whole volume of the cell or in selected regions of interest. ImageJ (http://imagej.nih.gov/ij/) and Photoshop (Adobe, San Jose, CA, USA) software were used for quantification of the fluorescence intensities of the complex, or to edit the images where appropriate. The calculation of average fluorescence intensity is illustrated in Figure 10.

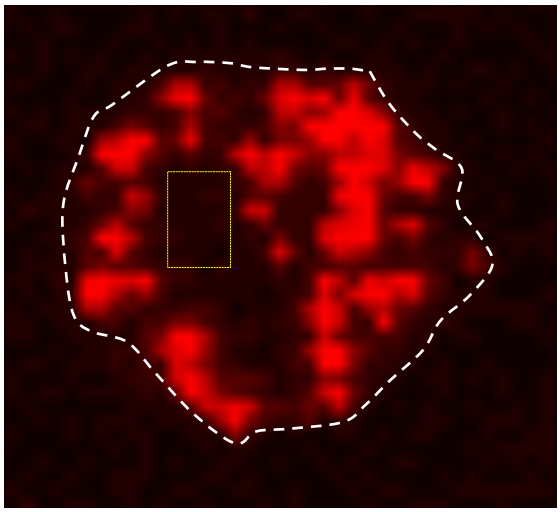

Figure 10. The calculation of the average complex fluorescence intensity in a cell
The cell is encircled by white dash line; this boundary was defined by the background area of pericentrin staining. The area encircled in yellow dash line serves as the 'noisy background' and was randomly selected within the cell boundary from the area lacking of complex PLA signal (red). The overall average intensity of the cell was calculated by subtracting the average intensity of the noisy background.

2.1.6 Routine immunofluorescence procedure

Immunofluorescence (IF) was used to detect the existence of the proteins of interest.

Blocking non-specific binding: Each coverslip with cells was transferred from 24 wells plates into a well of a 12 wells assay culture plate (Santa Cruz) on a preplaced parafilm disc. Cells were blocked using 25µl commercial PLA blocking solution at room temperature for 1 hour.

Primary antibody incubation: 20µl of 1:500 diluted primary antibody in PLA diluent was loaded onto each coverslip after removal of the PLA blocking solution using a strip of whatman paper, followed by incubation at 37°C for 120 minutes or overnight at 4°C.

Secondary antibody incubation: After washing with 1xPBS, 20µl secondary antibody solution in PLA diluent (1:500 dilution) were loaded onto the coverslips, followed by incubation at 37C for 1 hour.

DNA staining with DAPI: After washing with 1x PBS, 15µl DAPI (1:3000 diluted in PBS) was added to each coverslip, followed by incubation at room temperature for 15 minutes.

Mounting coverslips: After washing with 1 x PBS solution (2 x 5 minutes), the coverslips were dried on blue roll paper, and mounted on microscope slides (Academy

Science, Beckenham, UK) with 5ul mounting solution and sealed with nail glue. They were kept at 4℃ for use.

2.2 Western blot

2.2.1 Antibodies

Primary antibodies used for Western blot were same as those for Duolink PLA, listed in Table 1.

Secondary antibodies: IRDye 680RD donkey anti-rabbit IgG (H+L) (926–322227; LI-COR Biosciences) and IRDye 800CW donkey anti-mouse IgG (H+L) (926–32212; LI-COR Biosciences.

2.2.2 Reagents and Buffers

Lysis cocktail solution: CelLytic™ MT Cell Lysis Reagent (Sigma-Aldrich, C3228) containing 1x protease inhibitor cocktail (Sigma-Aldrich, p8340).

SDS-PAGE Loading buffer: 5x Laemli Buffer: 10 ml containing 0.5M Tris-HCL pH6.8, 45% Glycerol, 4.5ml SDS (0.25g dissolved in 1ml Tris-HCl), 2ml 0.5g total 0.25% Bromophenol blue (25mg in 10ml H_20), 0.5ml B mercaptoethanol, 1.25ml.

SDS-PAGE protein gel running buffer: 950ml deionized water + 50ml MOPS-SDS (RNAse free solution) running buffer (Formedium).

Transfer buffer: 25mM Tris Base (Sigma-Aldrich) +192mM Glycine (Sigma-Aldrich) +20% Methanol (Sigma-Aldrich) in deionized water.

Blocking solution: 1x PBS containing 1x Odyssey blocking buffer.

0.1% PBST: Tween-20 was prepared in 1x PBS.

2.2.3 Cells harvest and lysate preparation

After incubating for 24 hours (with or without drugs treatment), cells were trypsinized and transferred to a 15ml tube. After counting the cell population using a Nexcelom Auto T4 cellometer, the cell suspension was centrifuged (1000g, 4 minutes, 4℃), and then the pellet was washed gently with cold 1xPBS and kept on ice. The cell pellet was lysed with lysis cocktail solution (10^7 cells/ml) in a 1.5ml Eppendorf tube on ice for 30 minutes, with agitation, and then 5x loading buffer was added and heated at 99℃ for 10 minutes. The sample was then centrifuged at 12000g (4minutes at 4℃). The supernatant was transferred to a fresh tube and was kept at -20°C.

2.2.4 Western blot procedure

Running SDS-PAGE gel

Appropriate volumes of samples were loaded after adjustment according to the protein concentrations. 5µl standard Kaleidoscope pre-stained protein marker was also loaded.

The gel was run at 200 volts for 45-60 minutes.

Transferring the proteins to a nitrocellulose membrane

Once the SDS-PAGE was finished, the gel together with a piece of nitrocellulose membrane, was sandwiched by two pieces of whatman paper, plus sponges. The sandwich was placed in transfer buffer and the transfer was effected at 80 amps (A) for 1.5 hours.

Blocking non-specific binding

After transfer, the membrane was briefly washed with 1x PBS twice then blocked with 1x Odyssey blocking solution for 1 hour at room temperature, with gentle agitation.

Primary antibody incubation

The blocked membrane was incubated with primary antibody solution (1:500 in Odyssey blocking solution) at room temperature for 2 hours or kept at 4℃ overnight with agitation.

Secondary antibody incubation

After washing with 0.1% PBST (2 x 5 minutes), the membrane was incubated with the appropriate secondary antibody solution for 1 hour at room temperature with gentle agitation.

Detecting protein signals with Li-Cor Odyssey software

After incubating with the secondary antibodies and washing with 0.1% PBST, the membrane was scanned using Li-Cor Odyssey imaging system (Li-Cor, Lincoln, NE, USA). The 700nm channel was selected for detecting rabbit secondary antibodies in red, and the 800nm channel was selected for detecting mouse secondary antibodies in green, with appropriate intensity settings.

3. Results

3.1 Positive control PLA interaction using BUBR1 – MAD2

The successful completion of a PLA depends on a variety of parameters, such as the length of the incubations; the quality of the paired antibodies; the correct formulation of the buffers, and the sensitivity of the commercial product to being stored for a period of time. In order to test these factors the lab has previously established that a pair of antibodies for rabbit polyclonal anti-human Mad2 (Covance, PRB-452C) and mouse monoclonal anti-human BubR1 (Abcam, ab54894) will give strong fluorescent signals due to the protein-protein interactions between BubR1 and Mad2 (Figure 11) and this interaction is used as a positive control in each experiment. Where an experiment produced fluorescent signals that were weaker than those shown in figure 11 then that experiment was ignored.

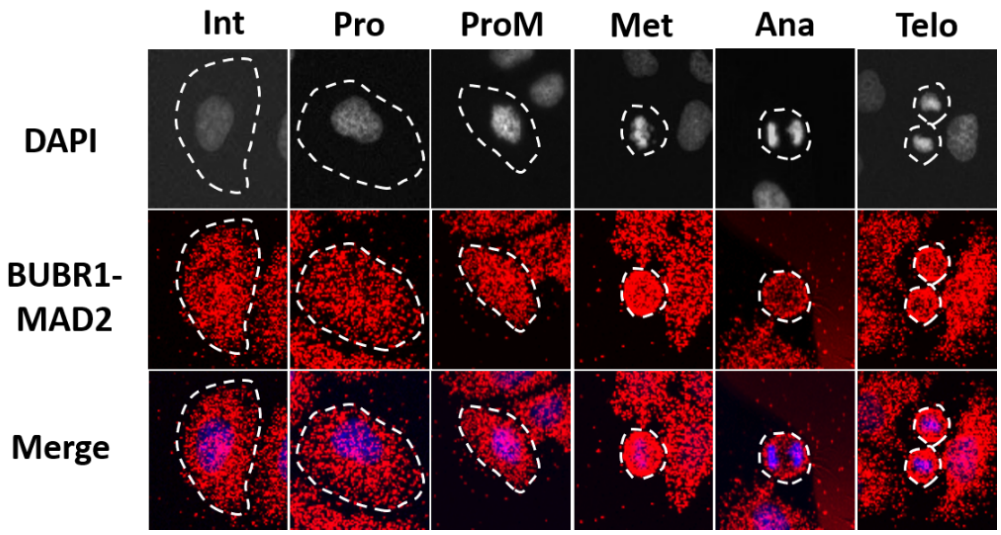

Figure 11. The interaction profiles of BubR1 and Mad2 as a PLA positive control
Projected images, from images acquired by confocal microscopy. The interaction profile of BubR1-Mad2 is shown qualitatively at interphase (Int), prophase (Pro), prometaphase (ProM), metaphase (Met), anaphase (Ana) and telophase (Telo) in HeLa Kyoto cells. The interaction between BUBR1 and MAD2 determined by the PLA fluorescence intensity is shown as red dots (excited at 549nm) with the cell boundaries indicated by white dashed lines. The DNA is stained with DAPI, shown in the top panel in grey and in blue in the bottom merged images (excited at 405nm). Cell cycle stages were determined by DNA morphology. The bottom panel shows a merged overlay, with DAPI in blue, and BubR1-Mad2 complex in red.

3.2 Comparison of performance between Hela B cell and Hela Kyoto cell

Our group has previously used HeLa cell subtype (HeLa B) for conducting the PLA for studying the protein-protein interaction between the proteins of interest but the HeLa

Kyoto despite of a bit over-populated (HeLa K hereafter) displayed more regular morphology than HeLa B, which could make the quantification and comparison easier. In order to determine if HeLa Kyoto cells would be behaved same as HeLa B cells from the prospective of PLA staining and could be used in this project, I performed experiments to test the quality of the outcome.

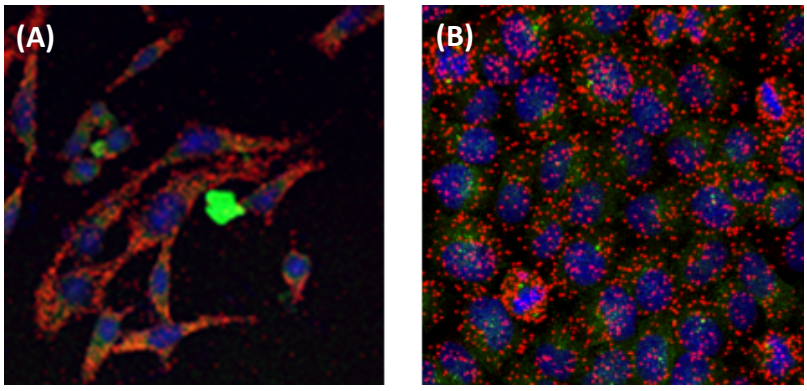

Figure 12. Staining HeLa B and HeLa K with BubR1 and Mad2 antibodies for comparison

Fixed HeLa B and HeLa K cells were stained with anti-BubR1 and anti-Mad2 antibodies for PLA as described in the materials and methods. The two confocal images shown were taken randomly. The left (A) image shows Hela B cells and the right one (B) shows Hela K cells. DNA stained with DAPI in blue, and the red dots indicate the BubR1-Mad2 protein complex. The distribution of red dots also indicates the rough shape of each cell. The green signals are centrosomes stained with anti-pericentrin antibody.

As can be seen in Figure 12. Hela B cells had an irregular shape, whereas Hela K cells were consistently smoother and more rounded in shape. Therefore, I chose to use Hela K cells for the remainder of the project.

3.3 Optimisation of PLA staining

At the beginning of this project, and over the subsequent 8 months, the PLA staining was found to be quite unstable, which caused significant obstacle for progressing the project. The PLA technique is operationally demanding and conditionally sensitive and during this period it has produced unexpected and confusing results. To solve this, I have tried to improve the protocol by optimizing the amount of the agents used for reaction, for instance I have increased the primary antibody dilutions from 1:500 to 1:200 based on the original commercial concentrations; and paying extra attentions to the steps where manipulation should be extremely cautious, or sterilization is prerequisite (the one outlined in the methods section), for instance, never apply the antibody solutions after the coverslips

were completely dried out. These efforts have significantly increased the success rate of PLA staining. The example confocal images were compared in Figure 13.

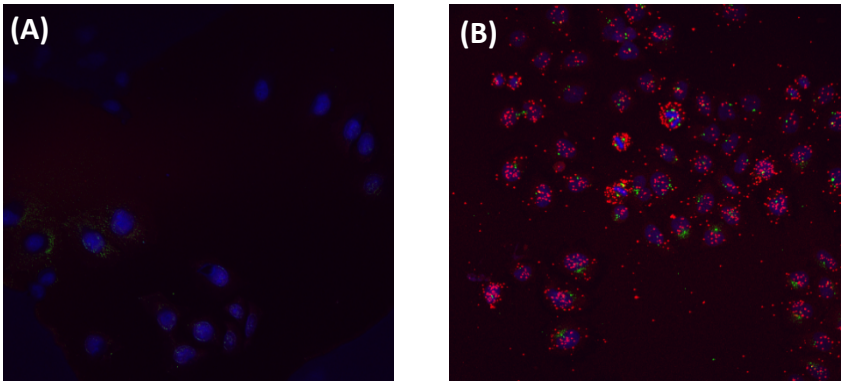

Figure 13. The comparison of HeLa K cells staining with the pair of antibodies against APC3 and CDC20 under different conditions

The two confocal images were randomly selected from two experiments following the previous protocol and modified protocol, respectively. The left image shows a typical staining where the PLA was failed (A); red signals, which represent the protein complex between APC3-CDC20 can hardly be detected. The right image show staining using optimised conditions (B), red signals are strong and clear. DNA stained with DAPI in blue and the centrosomes stained with anti-pericentrin in green.

3.4 Interaction between CDC20 and APC/C

As discussed in the introduction that the different components of the APC/C can bind to two CDC20 molecules at different time in mitosis for specification and targeting different substrates for destructions, for instance, the APC/C can be activated by binding to CDC20 with its APC8 subunit in early mitosis for targeting cyclin A for destruction in SAC-independent manner, while the SAC-dependent destruction of cyclin B1 and securin will require APC3 and APC8 interact with CDC20 (after liberated from MCC), and this process requires APC10 (refs). It is unclear if these two CDC20 molecules were interacted with the APC/C at the same time or at different time points in mitosis sequentially. In order to study the temporal profiles of these interactions, we investigated the protein-protein interaction profiles between APC3-CDC20, and APC8-CDC20, and as well as the interaction profiles between some components of the APC/C subunits.

3.4.1 Verification of antibody specificities

As the PLA assay uses two primary antibodies that are raised from different species, the specificity of these antibodies is crucial for the interpretation of the signals. All the antibodies used in this project were tested by pairing them with an appropriate random immunoglobulin G (IgG) and perform PLA staining, to act as a negative control. For example, polyclonal mouse anti-APC3 antibody was paired with a rabbit non-specific serum (random IgG (Figure 14).

In Figure 14, the red dots represent the non-specific signals produced between the APC3 antibody and a random IgG quantitatively, the intensity of for APC3-IgG remain at similarly low levels throughout the cell cycle stages (Figure 14). These signals are treated as the non-specific background. This non-specific background testing had applied to all antibodies used in this project where were appropriate. The specificity of the anti-CDC20 antibody has been tested previously in the lab (87).

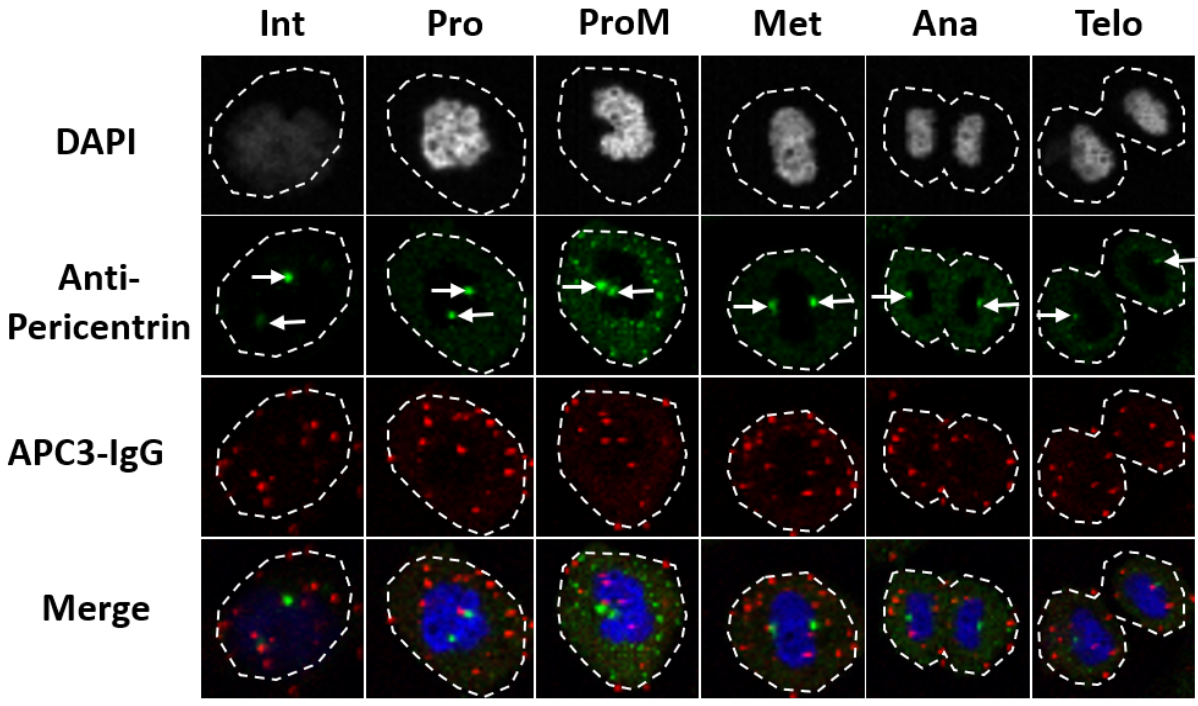

Figure 14. Testing the non-specific interaction between the anti-APC3 antibody and a random IgG
Example of projected Z-stack confocal images. The red fluorescent dots represent the qualitative levels of APC3-IgG throughout the selected cell cycle stages: interphase (Int), prophase (Pro), prometaphase (ProM), metaphase (Met), anaphase (Ana) and telophase (Telo). Cells are encircled by white dashed lines; the boundary is determined by the area of the non-specific green background produced centrosomes were stained with anti-pericentrin antibody. **Top panel**: DNA was stained with DAPI, shown in grey. **Middle panel 2**: The centrosomes were stained with anti-pericentrin antibody and FITC conjugated secondary antibody, green dots (highlighted by white arrows). The cemtrosome and DNA morphologies were used conjunctionally for

determining the cell stages. **Bottom panel**: Potential protein complex interactions between APC3-IgG were in red (594nm) and served as negative control.

3.4.2 The interaction profile between CDC20 and APC3

Therefore, the interaction profiles of APC3-CDC20 were analysed using PLA approach using above tested antibody pair.

Figure 15, example of Z-stack confocal images shows the APC3-CDC20 interaction profiles at the selected cell cycle stages qualitatively, the quantitative results were displayed (figure 16). The PLA fluorescent signals between APC3 and CDC20 were low in interphase and increased at prophase and peaked at metaphase before it was gradually declined in anaphase (Figure 16). This interaction profile before the metaphase is reflecting and agrees with previous findings, that the APC/C-CDC20 (MCC) is primarily in charge of the metaphase to anaphase transition and mitotic exit (14, 63). The declined interaction profiles of CDC20-APC3 at the end of mitosis, might resulted from the degradation of CDC20 targeted by the APC/C^{CDH1}

According to current knowledge, CDC20 are supposed to be degraded before telophase (60). However, as shown in figure 16 and 17, we still detect low level of APC3-CDC20 signal at the telophase above the non-specific background of APC3-Random IgG. This suggests that there were some CDC20 remained in the complex at this stage.

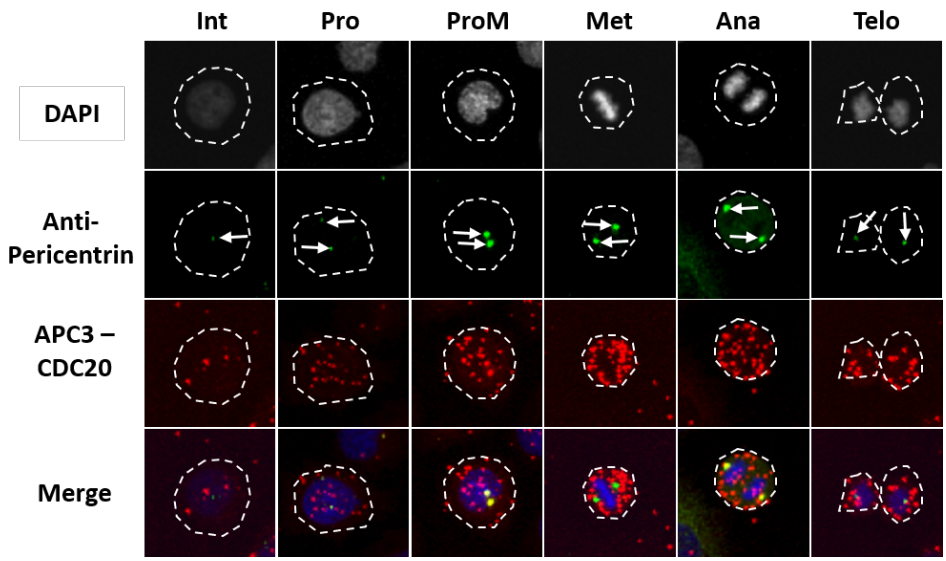

Figure 15. The interaction profiles of APC3 and CDC20 at the mototic stages of normal Hela cell cycle

Example of projected Z-stack confocal images. The red fluorescent dots represent the qualitative levels of APC3-CDC20 protein interaction at the selected cell cycle stages: interphase (Int), prophase (Pro), prometaphase (ProM), metaphase (Met), anaphase (Ana) and telophase (Telo). Cells are encircled with white dashed lines; the boundary is determined by the area of the non-specific green background produced by the centromeres stained with the anti-pericentrin antibody. Top panel: DNA was stained with DAPI, shown in grey~~scale~~ (405nm). Second top panel: the centrosomes were stained with the anti-pericentrin antibody and revealed by the FITC conjugated secondary antibody in green dots (488nm) and were highlighted by the white arrows. The centromes and DNA morphologies were conjunctionally used to determine the cell cycle stages. Third panel**:** The PLA signals of APC3-CDC20 in red (594nm). Bottom panel: The merged images, DNA (DAPI) in blue and the centrosomes (Pericentrin) in green, and the APC3-CDC20 protein complex in red.

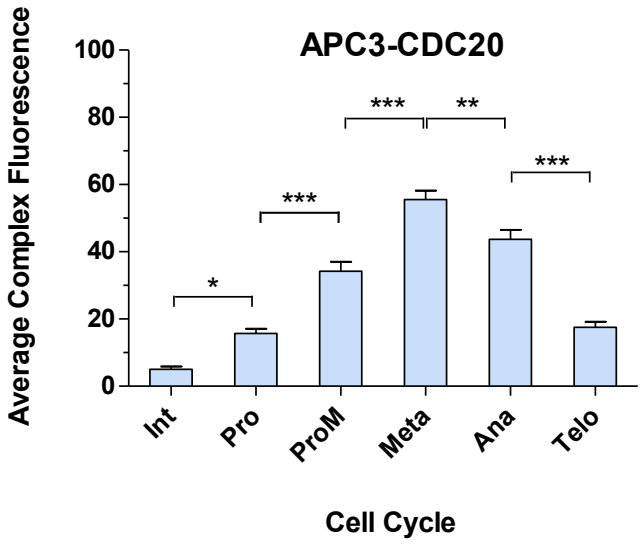

Figure 16. The quantitative interaction profiles of APC3 and CDC20 at the indicated cell cycle stages

The quantitative average maximum intensities of the PLA fluorescent signals of the APC3-CDC20 interactions across the cells at the interphase (Int), prophase (Pro), prometaphase (ProM), metaphase (Met), anaphase (Ana) and telophase (Telo). 10 cells from two independent experiments were quantified for each stage. Values on the vertical Y-axis show the average maximum intensities in (arbitrary units, (A.U.). Unpaired t-test were applied for statistical analysis, p value: * $p<0.05$, **: $p\leq0.001$, ***: $p<0.0001$. The fluorescent intensities were quantified from the projected Z-stack confocal images using ImageJ.

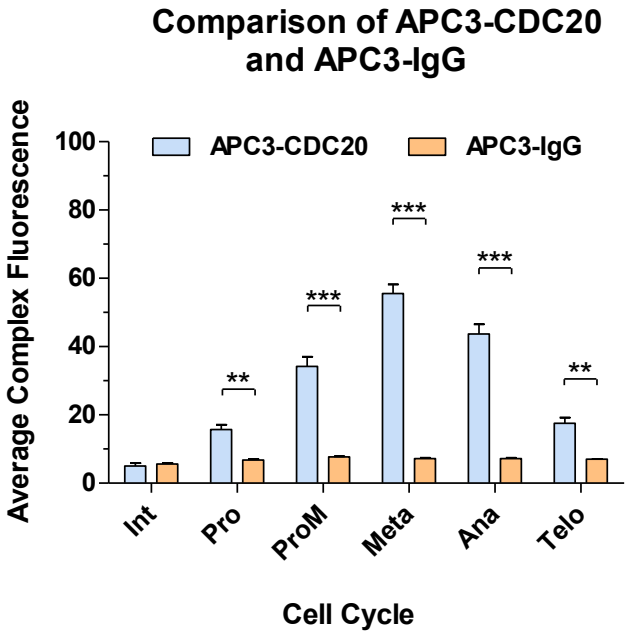

Figure 17. Quantitative results comparing the interaction profiles of APC3-IgG (negative control) and APC3-CDC20 throughout the cell cycle

The quantitative average maximum fluorescent intensities of the PLA signals between APC3-IgG (negative control, orange) and APC3-CDC20 (blue) at the cell cycle stages interphase (Int), prophase (Pro), prometaphase (ProM), metaphase (Met), anaphase (Ana) and telophase (Telo). 5 cells were quantified from each cell cycle

stages for APC3-IgG and 10 for APC3-CDC20 collectively from two independent experiments, under the same conditions. Values on the vertical Y-axis show the average maximum intensities displayed by arbitrary units, (A.U.). p value: **: p≤0.008, ***: p<0.0001. The fluorescent maximum intensities were quantified from the region of interests from the projected Z-stack confocal images using ImageJ.

3.4.3 Testing the PLA signals of APC3-CDC20 are genuinely reflecting the real interaction of APC3 and CDC20 using Apcin and TAME drug treatment.

To test if the PLA signals display and quantified in figure 16 & 17 reflect the genuine interaction of APC3-CDC20, two APC/C inhibitors, Apcin and tosyl-L-arginine methyl ester (TAME) (80, 81) were used for cell treatment prior to the PLA analysis. Apcin binds to the D-box motif to block the substrate interaction with CDC20 and TAME directly disrupts the interaction between APC3 and CDC20 (76, 81). Cells that have been treated with a mixture of the two drugs will be arrested effectively in metaphase, because the activity of the APC/C is abolished (80, 81) (Figure 18). As TAME will physically disrupt APC3-CDC20, we anticipate that the PLA signals between APC3-CDC20 will either be abolished, or significantly reduced in the presence of TAME.

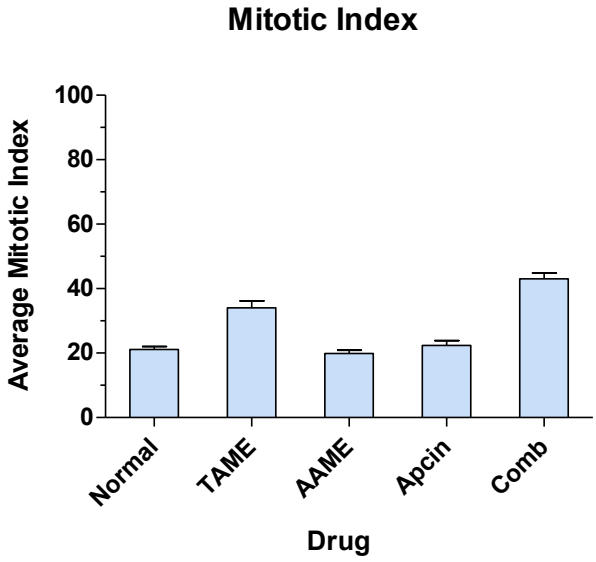

Figure 18. Comparison of the-mitotic indexes in HeLa cells after treated with drug as indicated for 24 hours

The mitotic index (%) (determined by rounded cell morphologies of the arrested cells), comb' = TAME + Apcin. 'normal'=untreated cells. 25mM of each drug was used for the treatments. The data were quantified from 6 repeat plates for each group. AAME (negative control): Acetyl-L-Arginine Methyl Ester.

The cells were treated with 25μM TAME, AAME, APCin, and the combined drugs of 25μM TAME+APCin and a normal control respectively for 24 hours. The total cells and the mitotic arrested cells with rounded up morphologies were counted under tissue culture microscope for calculating the mitotic index (Figure 18). Our results confirmed that AAME has no effect on the cell cycle progression of the HeLa cells compared with untreated (normal) cells under the condition as described (Figure 18). The cells after treated with 25μM APCin only caused marginally increase of the mitotic index. TAME has significantly increased the cells arrested in mitosis, but the largest increase was achieved by using the combined drugs (43% arrested cells). It was therefore the combined drug treatment was used to treat cells for PLA of APC3 and CDC20 interaction although we had not tried other conditions to achieve higher mitotic arrest of the cells due to the time limitation.

3.4.4 Quantitative analysis of the PLA fluorescent signals of APC3-CDC20 interaction after drug treatment

In order to determine if the PLA signals produced by the pair of antibodies against APC3 and CDC20 as shown above were genuinely reflecting the real dynamic interaction profiles of these two proteins throughout the cell cycle, we have performed experiments by treating the cells with or without (control) the combined drugs (25μM TAME+APCin). Unfortunately, the PLA staining with cells in control groups also shown negative results suggested that the staining processes of the PLA failed. Therefore, the efforts attempting to verify the genuine PLA signals was unsuccessful.

3.4.5 Western Blot examining the endogenous proteins of the APC/C components, CDC20 and Cyclin B1

Although above testing experiments using TAME and APCin drugs was unsuccessful, at the same time, we have also intended to examine the endogenous protein levels of the APC/C components and its co-activators, and substrates like CDC20 and Cyclin B1 by western blot experiments (figure 19).

Western blot was first performed using the cell extracts prepared from normal Hela Kyoto cells. Antibodies against APC3, APC8, CDC20, and Cyclin B1 were probed with the western blot membrane to reveal the endogenous protein levels. Cyclin B1 was also tested as the blockage of the APC/C activity, would block Cyclin B1 degradation.

The western blot results of APC3, APC8, CDC20 and Cyclin B1 are shown in Figure 19. A strong band was detected associated with CDC20 at the expected position of 55.4KD. A weaker band associate with APC3 at 100KD and a clear band at 76KD of APC8 were also detected. A weak band at 52.3KD (55KD?) was detected for Cyclin B1, at 52.3KD. Therefore, all the proteins of interest can be detected by western blot.

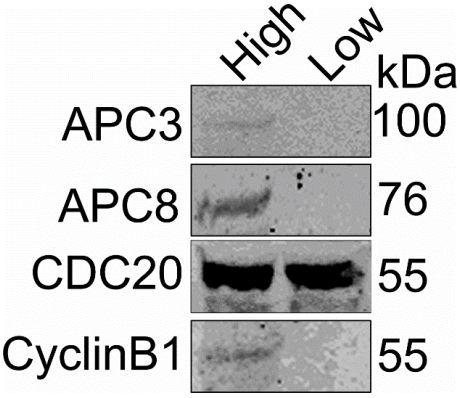

Figure 19. Western Blot for APC3, APC8, CDC20 and Cyclin B1 with the samples prepared from normal cell extracts

The bands for proteins of interests are shown, protein solutions with different concentration (1:500and 1:1000) were applied when loading the SDS gel, labelling High and Low in Figure 29.

Had established above western blot experimental conditions, we then examined the endogenous protein levels of APC3 and CDC20 under the treatment conditions as indicated (Figure 20). The western blot results shown that neither the levels of the endogenous APC3 nor CDC20 were affected by the treatments (Figure 20). Unfortunately, due to the time limitation we had not been able to repeat the PLA staining with the cells treated with the drugs to conceal a conclusive interpretation.

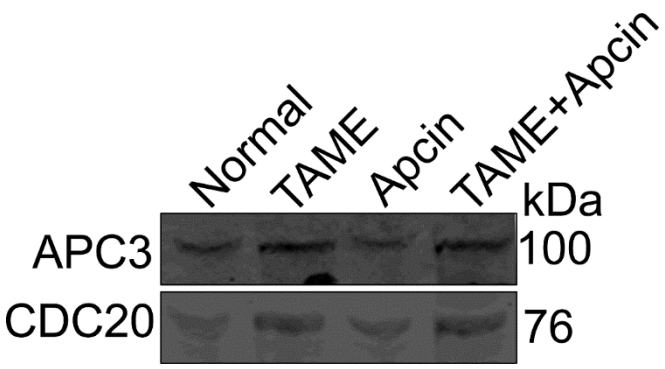

Figure 20. Western Blot comparing the endogenous levels of APC3 and CDC20 under normal and drug-treatment conditions

Cell extracts were prepared from Hela Kyoto cells after treated with or without 25mM TAME, Apcin and combined TAME + Apcin for 24 hours. the drug concentration for all three groups is 25uM. Normal cells of no drug treatment were used as control. The western blot membranes were probed with anti-APC3, and anti-CDC20 antibodies at dilution of 1:500.

3.4.6 The Interaction Profiles Between CDC20 and APC8

Following above of the quantification of APC3-CDC20, the APC8-CDC20 interaction profiles throughout the cell cycle stages were also tested to explore the differences between the two. The quantitative results are shown in Figure 21. The average maximum PLA fluorescence across each cell from projected Z-stack confocal images were quantified at interphase, prophase, prometaphase, metaphase, anaphase and telophase. The signal profile of ACP8-CDC20 interaction over the indicated cell cycle stages also displayed low level in interphase, and raised in prophase, but it has been noted to peak earlier than APC3-CDC20 at prometaphase and persisted the high level in metaphase before it was gradually declined in anaphase (Figure 21). Although it isn't directly comparable, but it has noted that the overall signal strengths of APC8-CDC20 is weaker than that of APC3-CDC20 (Figure 21), especially at metaphase stages. This became more obvious when the two set of data plotted together (Figure 22). This phenomenon might be due to this APC8 interacted CDC20 was pushed aside when the APC/C bound to the MCC (61) in prometaphase and metaphase weakened the PLA detection. Alternatively, it might suggest existing two different populations of the APC/C. Our results suggest that the interaction between APC3-CDC20 has been enhanced in prometaphase and metaphase.

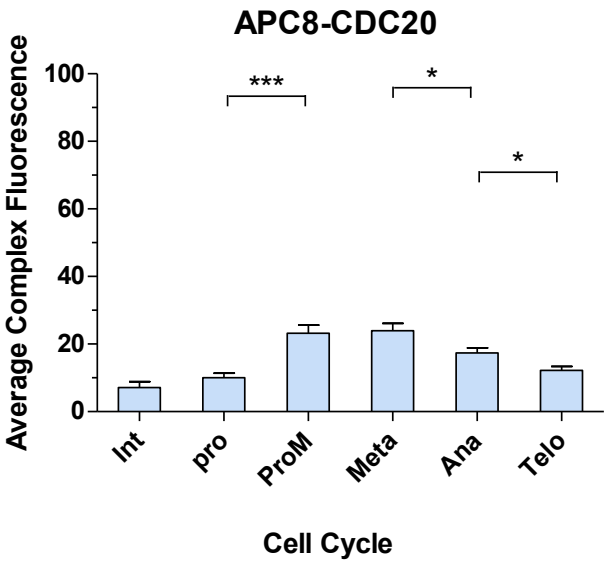

Figure 21. Quantitative interaction profiles of APC8-CDC20 throughout the cell cycle

The quantitative average maximum fluorescent intensities across cells of APC8-CDC20 at indicated cell cycle stages were quantified at interphase (Int), prophase (Pro), prometaphase (ProM), metaphase (Met), anaphase (Ana) and telophase (Telo). 10 cells from two independent experiments collectively were quantified for each stage. The values on the vertical Y-axis are the average maximum fluorescent intensities in arbitrary units (A.U.). p value: *: p≤0.02, ***: p<0.001. The maximum fluorescent intensities were quantified from the projected Z-stack confocal images using ImageJ.

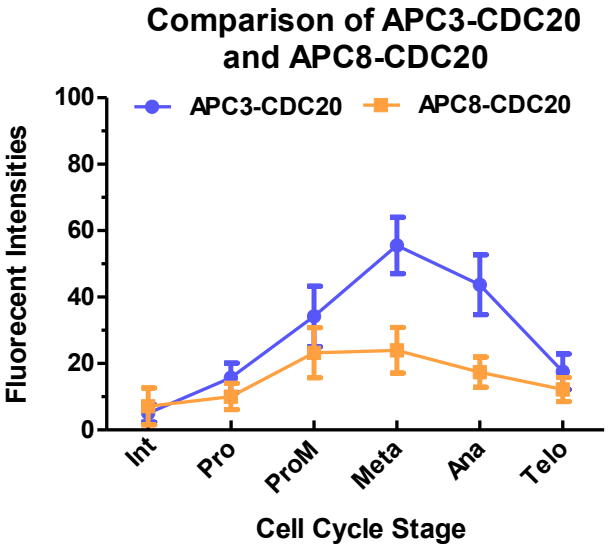

Figure 22. The comparison of the interaction profile between APC3-CDC20 and APC8-CDC20 over the phases of the cell cycle

The plots showing the average maximum fluorescent intensities across cells between APC3-CDC20 and APC8-CDC20 quantified from the projected Z-stack confocal images at interphase (Int), prophase (Pro), prometaphase (ProM), metaphase (Met), anaphase (Ana) and telophase (Telo). 10 cells collectively identified from two independent experiments were quantified for each stage as indicated. The values on the vertical Y-axis are the average maximum fluorescent intensities in arbitrary units (A.U.).

3.4.7 The Interaction Profiles Between CDC20 and APC11

APC3 and APC8 are both the components of the APC/C 'arc lamp' arm, and there are two copies of each in the APC/C (60). Our data suggest APC3 possess higher affinity with CDC20 than APC8 especially at metaphase, to rule out that this was not caused by the existing two populations of the APC/C, it is necessary to test the interaction between CDC20 and other APC/C subunits.

APC11 is catalytic subunit that regulates the interface of APC/C with E2 enzymes (60). We reasoned that it should maintain interact with CDC20 whenever CDC20 activates APC/C regardless if it was from $CDC20^{APC8}$ in prophase or $CDC20^{MCC}$ in prometaphase and metaphase (64). If this would be the case, we would then anticipate to detect persistent relatively high levels throughout the prophase to metaphase similar to the situation observed between APC3-CDC20 in prometaphase and metaphase if this is only one APC/C, otherwise, the level of APC11-CDC20 at prophase might different to the levels at prometaphase and metaphase.

The quantitative and comparison results of the profile of the average maximum intensities of APC11-CDC20 PLA signals at the indicated cell cycle stages are shown in Figure 23 & 24. The preliminary results noted interestingly that the interactions between APC11-CDC20 at prometaphase and metaphase are significantly higher than the levels at prophase, which might suggest in favour of existing different populations of the APC/C. However, this interpretation was complicated and become difficult by the observation the interaction between APC11 and CDC20 remained unexpected high levels at anaphase and lasted into telophase when the CDC20 supposed to be degraded (63, 64) (Figure 23 & 24). The APC/C catalytic sub complex contains 3 APC/C subunits which are APC2, APC10 and APC11, it would be important to test the interaction between APC2-CDC20 or APC10-CDC20 for comparison. It will be also interesting to test exactly what levels of the endogenous CDC20 remained at anaphase and telophase, and if this residue levels of CDC20 would interact with APC11. We cannot rule out that this was caused by non-specific interactions. Unfortunately, there was no anti-APC2 antibody available in the lab at the time when the project was conducted, and the experiments of assaying APC10-CDC20 fail due to technical issues.

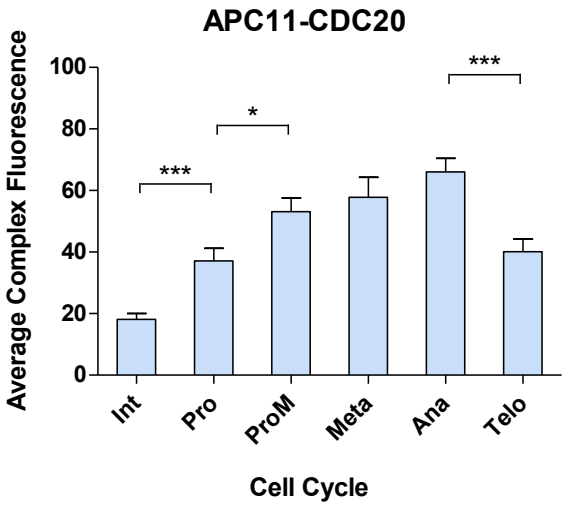

Figure 23. Quantitative results showing the profiles of APC11-CDC20 throughout the cell cycle

The quantitative average maximum fluorescent intensities across cells of APC11-CDC20 at indicated cell cycle stages were quantified at interphase (Int), prophase (Pro), prometaphase (ProM), metaphase (Met), anaphase (Ana) and telophase (Telo). 10 cells from two independent experiments collectively were quantified for each stage. The values on the vertical Y-axis are the average maximum fluorescent intensities in arbitrary units (A.U.). p value: * $p<0.01$, ***: $p<0.001$. The maximum fluorescent intensities were quantified from the projected Z-stack confocal images using ImageJ.

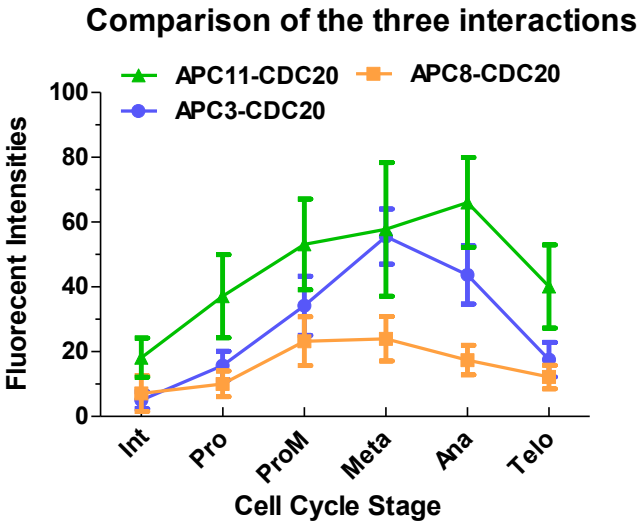

Figure 24. The comparison of the interaction profile between APC3-CDC20, APC8-CDC20, and APC11-CDC20 over the phases of the cell cycle

The quantitative average maximum fluorescent intensities across cells of APC3-CDC20, APC8-CDC20, and APC11-CDC20 at indicated cell cycle stages were quantified at interphase (Int), prophase (Pro), prometaphase (ProM), metaphase (Met), anaphase (Ana) and telophase (Telo). 10 cells from two independent experiments collectively were quantified for each stage. The values on the vertical Y-axis are the average maximum fluorescent intensities in arbitrary units (A.U.). The maximum fluorescent intensities were quantified from the projected Z-stack confocal images using ImageJ.

3.5 Insights into the in vivo assembly of the APC/C

3.5.1 The interaction profile of APC3 and APC6

As mentioned above, the APC/C is a large multiple subunits protein complex containing three functional domains as discussed in the introduction, the platform, TPR lobe (or arc lamp) and the catalytic domains (reviewed in 63). Resembling the SCF, the Cullin-like subunit APC2, the Ring finger protein APC11 and E2 enzymes comprise the minimal catalytic function of substrate ubiquitination (65). The TPR lobe contains APC6/Cdc16, APC8/Cdc23, APC3/Cdc27 and APC7 APC13, APC16 and Cdc26 subunits which provides binding sites for the platform subunit and the interaction interface for its co-activators, CDC20 and Cdh1, as well as regulation roles (Reviewed in 63). Its functional activities were regulated throughout the cell cycle selectively targeting substrates for ubiquitination hence degradation (reviewed in 63). However, exactly how the APC/C assembled in vivo, and if the dynamic components of the TPR arm were uniformly associate with the APC/C for function remained unanswered. The regulation the functions of the APC/C partly achieved by selectively interact with its co-activators and inhibitors at different time and space within the cell at different cycle stages, It has been suggested that there might exist sub-complexes of the APC/C in Drosophila (86), in order to shed light on this, we have selected and studied the cell cycle profiles of the interactions between APC3 (Cdc27) and APC6 (Cdc16), and APC3 and APC10 in HeLa cells. APC3 and APC6 are both the components of the TPR arm and APC10 is belonging to the catalytic domain, we were examining the dynamic interactions of APC3 and APC6 throughout the cell cycle; and hoping to reveal when the domain proteins interacted.

The quantitative results of the average maximum intensities showing the interaction profiles between APC3-APC6 were shown in figure 25. The signal profile of the interaction between APC3 and APC6 shown relative low level in interphase and declined in telophase (Figure 25) but remained relative high-level interaction in mitosis from prophase to metaphase (Figure 25).

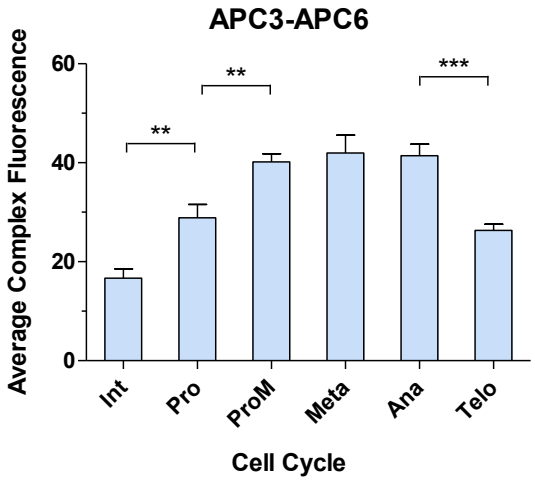

Figure 25. Quantitative results showing the interaction profile of APC3-APC6 throughout the cell cycle

The quantitative average maximum fluorescent intensities across cells of APC3-APC6 at indicated cell cycle stages were quantified at interphase (Int), prophase (Pro), prometaphase (ProM), metaphase (Met), anaphase (Ana) and telophase (Telo). 10 cells from two independent experiments collectively were quantified for each stage. The values on the vertical Y-axis are the average maximum fluorescent intensities in arbitrary units (A.U.). p value: **: $p \leq 0.02$, ***: $p < 0.001$. The the maximum fluorescent intensities were quantified from the projected Z-stack confocal images using ImageJ.

3.5.2 The interaction profile of APC3 and APC10

Figure 26 and 27 showing the quantitative dynamic interaction profiles of APC3-APC10 at the indicated cell cycle stages. As these proteins belong to the TPR sub-complex and catalytic core sub-complex, the interaction profile could provide insight into how the two sub-complexes were assembled. The results suggest that there was only basal level interaction between APC3 and APC10 in interphase, the interactions occurred when cell enter prophase and this was steadily increased till metaphase, and surprisingly, the interaction seems rapidly declined after metaphase anaphase transition (figure 26, 27).

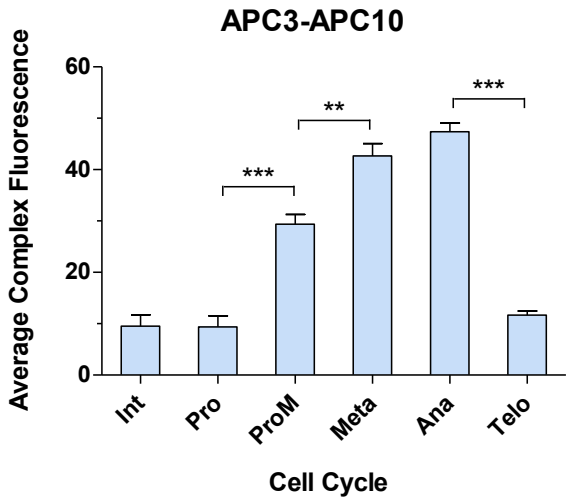

Figure 26. Quantitative results showing the interaction profile of APC3-APC10 throughout the cell cycle

The quantitative average maximum fluorescent intensities across cells of APC3-APC10 at indicated cell cycle stages were quantified at interphase (Int), prophase (Pro), prometaphase (ProM), metaphase (Met), anaphase (Ana) and telophase (Telo). 10 cells from two independent experiments collectively were quantified for each stage. The values on the vertical Y-axis are the average maximum fluorescent intensities in arbitrary units (A.U.). p value: **: p≤0.004, ***: p<0.001. The maximum fluorescent intensities were quantified from the projected Z-stack confocal images using ImageJ.

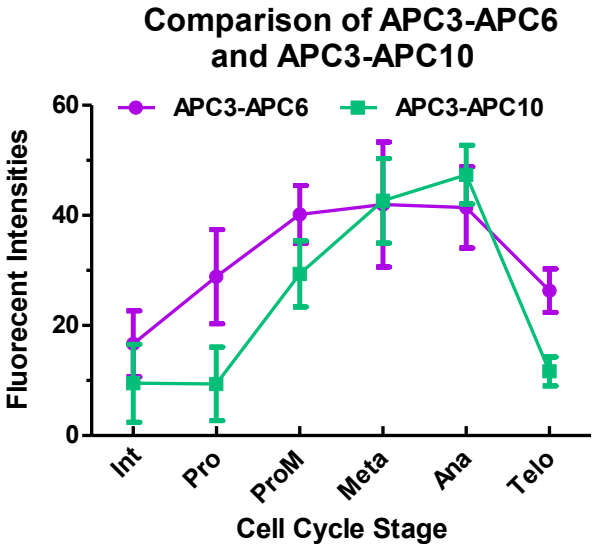

Figure 27. The comparison of the interaction profile between APC3-APC6 and APC3-APC10 over the phases of the cell cycle

The quantitative average maximum fluorescent intensities across cells of APC3-APC6 and APC3-APC10 at indicated cell cycle stages were quantified at interphase (Int), prophase (Pro), prometaphase (ProM), metaphase (Met), anaphase (Ana) and telophase (Telo). 10 cells from two independent experiments collectively were quantified for each stage. The values on the vertical Y-axis are the average maximum fluorescent intensities in arbitrary units (A.U.). The the maximum fluorescent intensities were quantified from the projected Z-stack confocal images using ImageJ.

DISCUSSION

The development and survival of eukaryotic organisms relies on cell division. Accurate chromosome segregation at the end of mitosis is critical for maintaining genome stability and inheritance. Mis-segregation of chromosome during mitosis can lead to some genetic disorders, like Down syndrome, birth defects and even cancers (1-5). The spindle assembly checkpoint (SAC) is the most important mechanism in mitosis which monitors the segregation of the sister-chromatids and delays mitotic procession so that errors can be corrected when it is appropriate (6, 7).

The SAC functions to prevent the premature sister-chromatid segregation - at anaphase onset by inhibiting the premature activation of the activity of the anaphase promoting complex/cyclosome (APC/C) by its coactivator CDC20 (cell division cycle protein 20) (6, 8). The APC/C is a large multi-subunits protein complex which functions as an E3 ubiquitin ligase and targets substrates by ubiquitination and consequently destruction by the proteasome throughout the cell cycle (reviewed in 61). It contains three functional subdomains: the scaffolding platform consists of APC1, APC4, and APC5 components; the catalytic domain consists of APC2 (a Cullin family related protein), APC10 (Doc1) and APC11 (RING finger protein); and the TPR (tetratricopeptide repeat) lobe domain consists of APC3, APC6, APC7, APC8, APC13, APC16 and Cdc26 subunits (Reviewed in 63). The spatiotemporal activation of the APC/C is primarily achieved by sequential and regulated binding to its two co-activators, CDC20 and Cdh1 leading to the formation of APC/C^{CDC20} and APC/C^{Cdh1} which are two E3 ligase complexes (Reviewed in 61). The APC/C^{CDC20} primarily controls the metaphase/anaphase transition and mitotic exit by targeting Cyclin B1 and securin destructions through regulation by the SAC (Reviewed in 61). The SAC inhibitory signal is mainly cascaded onto the unattached kinetochores to produce diffusible a “anaphase waiting” signal, which refers to a four-protein complex, the mitotic checkpoint complex (MCC) (Reviewed in 63). The MCC is formed from two sub-complexes of BubR1-Bub3 and Mad2-CDC20 (Reviewed in 62) and its function is to inhibit the APC/C^{CDC20} to prevent the premature degradation of Cyclin B1 and securin until all the kinetochores have achieved the amphitelic microtubule attachments that satisfy the SAC (Reviewed in 62). However, the APC/C^{CDC20} can also target other substrates, such as Nek2A and Cyclin A which are degraded

in prometaphase independently of the SAC (64). The APC/C^{Cdh1} however mainly functions during the end of mitotic exit and in the G1 phase (20).

In late mitosis, the APC/C^{Cdh1} targets substrates like Aurora A and UBCH10, PLK1, CDC20 itself and many others for destruction (18, 20), although CDH1 is not essential for some species (21). However, exactly how the APC/C^{CDC20} can target Nek2A and Cyclin A for destruction independently of the SAC and target the securin and Cyclin B1 for destruction under the SAC regulation was not fully understood until recently. Izawa and Pines (13) have shown that a new CDC20 can interact with different components of the APC/C, APC3 and APC8 in prophase and metaphase, to specify cyclin A and cyclin B for ubiquitination and hence degradation (20). At the same time the MCC can also inhibit this new CDC20, which has already bound to and activated the APC/C to prevent cyclin B1 and securin destructions (13). The destructions of cyclin B1 and securin require CDC20 interaction with APC3 and APC8 and also require APC10 (Doc1), whereas it only need to bind to APC8 for Cyclin A destruction (13). However, the dynamic interactions of CDC20 and the components of the APC/C have never been studied in vivo during the cell cycle; so there is no information available about whether $CDC20^{APC8}$ and $CDC20^{MCC}$ are bound to the APC/C at the same time or whether they bind sequentially; and there is a complete lack of information about the dynamic assembly of the APC/C throughout the cell cycle. In this project we provide some preliminary results which give some insights into these problems.

We have used the Duolink based proximity ligation assay to study the in vivo protein-protein interactions between APC3-CDC20, APC8-CDC20, and APC11-CDC20 intended to examine the interactions between CDC20 and the APC/C and also examined the dynamic assembly of the APC/C by looking at APC3-APC6, and APC3-APC10 complexes.

The Duolink PLA technique utilizes two primary antibodies raised in different animal species for targeting two different proteins of interest in fixed individual single cells (http://www.olink.com/products/duolink/applications/protein-interactions). A pair of species-specific PLA probes conjugated with unique short oligonucleotide tails, bind to the primary antibodies and act as a template when the two PLA probes are in close proximity (< 40 nm) for rolling circle amplification to incorporate fluorescent labeled oligonucleotides into the products. This amplified fluorescent signal can be detected and quantified based on microscopy images (80). Thus the PLA technique has some unique and irreplaceable

characteristics, for instance, it is one of a few widely used and commercially available methods for analysing protein-protein interactions in their native state suing individual single cells (77), and as such it avoids biochemical extraction or the creation of exogenous over-expressed fusion proteins, and can assign signals to specific subcellular locations, although it might not provide sufficient accuracy to localize the signals to superstructures like the kinetochores (81). However, the successful completion of an assay depends on a variety of factors as it requires multiple steps and having a positive control is extremely important, and attention to detail at all steps is essential. As the PLA merely indicates when the two proteins of interest are within 40nm of each other (80) proving that that the interaction of the two proteins is genuine requires verification by other means (80). In this project, the specificities of all the antibodies used were tested by pairing with an appropriate random IgG either by myself or by other lab members and these will serve as the negative control. An example of the negative control confocal images between APC3-Random IgG and the relevant quantitative results were shown in Figure 14 & 16 respectively. As a result of the test, by comparing to the negative control, the dynamic PLA signals produced between APC3-CDC20 at the indicated cell cycle stages are less likely of non-specific consequence (figure 14 & 16). We have performed experiments to test if these PLA signals reflect the genuine dynamic interactions of AOC3 and CDC20 at the cell cycle indicated using two APC/C inhibitors. TAME (tosyl-L-arginine methyl ester) has been proved to physically disrupt the interaction between APC3 and CDC20 (84). AAME (Acetyl-L-Arginine Methyl Ester), a non-functional analogous of the TAME was used as the negative control (85). APCin is an inhibitor preventing the interaction between CDC20 and the substrate, such as lCyclin B1 (85). It has been suggested that the cells treated with the combined drugs of TAME and APCin will cause the highest mitotic arrest (85). 25μM of each drug was used either singly or combined for treating the cells (Figure 18), although we have not achieved high percentage mitotic arrest (>80%), but we do confirmed that the combined drugs between TAME and APCin can cause highest mitotic arrest compared with the mitotic index resulted from other groups (figure 18). Although we have seen very low PLA signals of APC3-CDC20 after the cells were treated with the combined drugs, unfortunately the PLA staining from the samples of the parallel control was unsuccessful, we have been unable to draw a conclusion on the attempt to verify the PLA signals between APC3-CDC20 (figure 16). Due to the time limitation, the repeat experiments had not been performed. As there were no

other drugs available could be used to verified the other pair protein-protein interactions, for instance, APC8-CDC20, APC11-CDC20, APC3-APC6 etc., at the same time, we had also attempt to establish siRNA experimental condition to transiently knockout the protein of interest from the culture cells as an alternative approach to test the genuine interactions between APC3 and CDC20 reflected by the PLA signal The preliminary results showing that we have successfully depleted APC3 and CDC20 from the HeLa cells revealed by western blot (Figure 20). Unfortunately, the time had run out for me to perform new experiments to conduct PLA staining of APC3-CDC20 after siRNA to knockout the proteins of interest, and this remained as one that must be performed if I could have more time in the future.

Despite of the uncompleted or unsuccessful for the verification of the genuine PLA signals for the interaction profiles of the protein of interests, by comparing PLA signals at the indicated cell cycle stages which potentially reflect the interaction profiles between the protein pairs of APC3-CDC20, and APC8-CDC20, it still provides some new insights into the spatiotemporal interactions for understanding how might the APC/C were regulated in terms of the interaction with its co-activator of CDC20. It used to known that the function of CDC20 as the APC/C coactivator will be sequestered by the SAC by integrated into the MCC (mitotic checkpoint complex, containing BubR1, Bub3, CDC20 and MAD2) before anaphase onset (78). However, the APC/C is not fully silenced when the SAC is on in late prophase and early prometaphase, and is able to target Nek2A and Cyclin A for degradation, and the APC/C can only target cyclin B1 and securin for destructions at the end of the mitosis (60). It has been suggested that the APC/C change its substrates specificity by binding to a second CDC20, this second CDC20 interacts with APC8 of the APC/C and activate the APC/C and targets Nek2A and Cyclin A for ubiquitination hence destruction (61). This second CDC20 can also be inhibited by the MCC, and the destructions of Cyclin B1 and securin will require CDC20 interacts with APC3 and APC8, and the processes requires APC10 (Doc1) too (61). However, the in vivo spatiotemporal interaction of CDC20 with the APC/C has never been revealed, and the two CDC20 ($CDC20^{APC8}$ and $CDC20^{MCC}$ were interacted with the APC/C at the same time or at the different time point in the mitosis remained elusive. In this project, by comparing the interactions cell cycle profiles between APC3-CDC20 ($CDC20^{MCC}$) and APC8-CDC20 ($CDC20^{APC8}$) (Figure 20), the overall signal strengths of the APC8-$CDC20^{APC8}$ are weaker than that of APC3-$CDC20^{MCC}$; the interaction between APC8-$CDC20^{APC8}$ peaked at

prometaphase, and APC3-CDC20^{MCC} peaked at metaphase. These preliminary results could be interpreted as that CDC20^{APC8} interacts with the APC/C earlier than that of CDC20^{MCC}. To test this, we studied the interaction profiles of APC11-CDC20, we reasoned that, if APC11-CDC20^{APC8}, and APC11-CDC20^{APC3} interacted at the same time, we would expect to see a same strength interaction signals at prometaphase and metaphase, otherwise, APC11-CDC20^{APC3} should be higher the same as observed for APC3-CDC20^{MCC} (Figure 20). Although we had unexpectedly detected a strong signal of APC11-CDC20 at anaphase, there is no significant different between PLA signals of APC11-CDC20 at prometaphase and metaphase. This suggests that APC11-CDC20^{APC8}, and APC11-CDC20^{APC3} interacted at the same time, and in favour the interpretation of that there is only one APC/C (Figure 21).

The APC/C is a large multi-subunits E3 ubiquitin ligase and is functioning throughout the cell cycle under regulation by its inhibitors, such as Emi1 in S phase and MCC in mitosis (21), and its co-activator, CDC20 in mitosis and Cdh1 in G1/S phases (21). Human APC/C comprising 14 distinct proteins of 19 components (34), it consists of scaffolding platform domain comprising of APC1, APC4 and APC5; the catalytic domain composed of APC2, APC10 and APC11; the TPR (tetrapeptiderepeat) arm domain, consisting of APC3, APC6, APC7, and APC8 etc. (Reviewed in 61). The TPR arm is also important as the scaffolding and stabilizing the APC/C as well as regulatory roles (Reviewed in 61). However, whether all these components were required at the same time, and how the APC/C was assembled in vivo of the cells remained largely unknown. The components of the APC/C studied in this project, APC3, APC6, APC8 are belonged to the TPR domain and APC10 and 11 are the core components of the catalytic domain. We have therefore studied the interaction profiles between APC3-CDC6 and APC3-APC10 to study if the components of APC3 and APC6 are always stay together or not as it has been shown that CDC27(APC3) and CDC16 (APC6) in Drosophila could differentially localised in mitosis (64). APC3 and APC10 are associate with the two different functional domains of the APC/C, the PLA signals of APC3-APC10 could provide insights into the dynamic assembly of the APC/C in the cell cycle.

The quantitative results shown by the figure 25, the APC3-APC6 interaction is cell cycle regulated, it stays low in interphase and increases in prophase and reached the peak and persistent at high level throughout prometaphase, metaphase and anaphase, and declined in telophase. In contrast to the APC3-APC6, the preliminary interaction profiles of

APC3-APC10 remained low in interphase and prophase, the interaction was significantly increased in prometaphase, and was continuing to increase till to the anaphase, and then it was dramatically reduced in telophase. These observations might suggest that the two functional domains of the APC/C, the TPR arm and the catalytic domain, might only assembled in late prophase and in prometaphase, or alternatively, the interactions of APC3 and APC10 on the APC/C are only accessible for detection by around prometaphase due to the conformational changes of the APC/C when it bound to the MCC (34). We understand our results are preliminary observations, and they are yet to be further tested in the future.

References

1. Holland AJ. Chromosomal instability, aneuploidy and tumorigenesis. 2009.
2. Bharadwaj R. The spindle checkpoint, aneuploidy, and cancer. 2004.
3. Ricke RM. Aneuploidy in health, disease, and aging. J Cell Biol. 2013.
4. Silk AD, Zasadil LM, Holland AJ, Vitre B, Cleveland DW, Weaver BA. Chromosome missegregation rate predicts whether aneuploidy will promote or suppress tumors. Proc Natl Acad Sci U S A. 2013 Oct 29;110(44):E4134-41. PubMed PMID: 24133140. Pubmed Central PMCID: 3816416.
5. Zasadil LM, Britigan EM, Weaver BA. 2n or not 2n: Aneuploidy, polyploidy and chromosomal instability in primary and tumor cells. Semin Cell Dev Biol. 2013 Apr;24(4):370-9. PubMed PMID: 23416057. Pubmed Central PMCID: 3736819.
6. Lara-Gonzalez P, Westhorpe FG, Taylor SS. The spindle assembly checkpoint. Curr Biol. 2012 Nov 20;22(22):R966-80. PubMed PMID: 23174302.
7. Musacchio A, Salmon ED. The spindle-assembly checkpoint in space and time. Nat Rev Mol Cell Biol. 2007 May;8(5):379-93. PubMed PMID: 17426725.
8. Yu H. Regulation of APC-Cdc20 by the spindle checkpoint. Curr Opin Cell Biol. 2002 Dec;14(6):706-14. PubMed PMID: 12473343.
9. Santaguida S AA. Short- and long-term effects of chromosome mis-segregation and aneuploidy. Nat Rev Mol Cell Biol. 2015:473-95.
10. Bharadwaj R, Yu H. The spindle checkpoint, aneuploidy, and cancer. Oncogene. 2004 Mar 15;23(11):2016-27. PubMed PMID: 15021889.
11. A A. Down syndrome - A Narrative Review. 2015.
12. Rieder CL, Schultz A, Cole R, Sluder G. Anaphase onset in vertebrate somatic cells is controlled by a checkpoint that monitors sister kinetochore attachment to the spindle. J Cell Biol. 1994 Dec;127(5):1301-10. PubMed PMID: 7962091. Pubmed Central PMCID: 2120267.
13. Porter LA, Donoghue DJ. Cyclin B1 and CDK1: nuclear localization and upstream regulators. Prog Cell Cycle Res. 2003;5:335-47. PubMed PMID: 14593728.
14. Gavet O, Pines J. Progressive activation of CyclinB1-Cdk1 coordinates entry to mitosis. Dev Cell. 2010 Apr 20;18(4):533-43. PubMed PMID: 20412769. Pubmed Central PMCID: 3325599.
15. Gavet O, Pines J. Activation of cyclin B1-Cdk1 synchronizes events in the nucleus and the cytoplasm at mitosis. J Cell Biol. 2010 Apr 19;189(2):247-59. PubMed PMID: 20404109. Pubmed Central PMCID: 2856909.
16. Nasmyth K, Haering CH. Cohesin: its roles and mechanisms. Annu Rev Genet. 2009;43:525-58. PubMed PMID: 19886810.
17. Mehta GD, Rizvi SM, Ghosh SK. Cohesin: a guardian of genome integrity. Biochim Biophys Acta. 2012 Aug;1823(8):1324-42. PubMed PMID: 22677545.
18. Pines J. Cubism and the cell cycle: the many faces of the APC/C. Nat Rev Mol Cell Biol. 2011 Jul;12(7):427-38. PubMed PMID: 21633387.
19. Castro A, Bernis, C., Vigneron, S. The anaphase-promoting complex: a key factor in the regulation of cell cycle. Oncogene. 2005.
20. Izawa D, Pines J. How APC/C-Cdc20 changes its substrate specificity in mitosis. Nat Cell Biol. 2011 Mar;13(3):223-33. PubMed PMID: 21336306. Pubmed Central PMCID: 3059483.
21. Blanco MA S-DA, de Prada JM, Moreno S. APC(ste9-srw1) promotes degradation of

mitotic cyclins in G(1) and is inhibited by cdc2 phosphorylation. The EMBO. 2000.
22. Nakayama K, Nagahama, H., Minamishima, Y.A., Matsumoto, M.,, Nakamichi I, Kitagawa, K., Shirane, M., Tsunematsu, R., Tsukiyama, T.,, Ishida N. Targeted disruption of Skp2 results in accumulation

of cyclin E and p27(Kip1), polyploidy and centrosome overduplication. EMBO J. 2006.
23. Acquaviva C, Herzog F, Kraft C, Pines J. The anaphase promoting complex/cyclosome is recruited to centromeres by the spindle assembly checkpoint. Nat Cell Biol. 2004 Sep;6(9):892-8. PubMed PMID: 15322556.
24. Reverend Dr John Wilson TH. Molecular Biology of the Cell, the 5th Edition2008.
25. Mimori-Kiyosue Y, Tsukita S. "Search-and-capture" of microtubules through plus-end-binding proteins (+TIPs). J Biochem. 2003 Sep;134(3):321-6. PubMed PMID: 14561716.
26. Biggins S, Walczak CE. Captivating capture: how microtubules attach to kinetochores. Curr Biol. 2003 May 27;13(11):R449-60. PubMed PMID: 12781157.
27. London N, Biggins S. Signalling dynamics in the spindle checkpoint response. Nat Rev Mol Cell Biol. 2014 Nov;15(11):736-47. PubMed PMID: 25303117. Pubmed Central PMCID: 4283840.
28. Foley EA, Kapoor TM. Microtubule attachment and spindle assembly checkpoint signalling at the kinetochore. Nat Rev Mol Cell Biol. 2013 Jan;14(1):25-37. PubMed PMID: 23258294. Pubmed Central PMCID: 3762224.
29. Jia L, Kim S, Yu H. Tracking spindle checkpoint signals from kinetochores to APC/C. Trends Biochem Sci. 2013 Jun;38(6):302-11. PubMed PMID: 23598156.
30. Suryadinata R, Sadowski M, Sarcevic B. Control of cell cycle progression by phosphorylation of cyclin-dependent kinase (CDK) substrates. Biosci Rep. 2010 Aug;30(4):243-55. PubMed PMID: 20337599.
31. Brandeis M, Rosewell I, Carrington M, Crompton T, Jacobs MA, Kirk J, et al. Cyclin B2-null mice develop normally and are fertile whereas cyclin B1-null mice die in utero. Proc Natl Acad Sci U S A. 1998 Apr 14;95(8):4344-9. PubMed PMID: 9539739. Pubmed Central PMCID: 22491.
32. Draviam VM, Orrechia S, Lowe M, Pardi R, Pines J. The localization of human cyclins B1 and B2 determines CDK1 substrate specificity and neither enzyme requires MEK to disassemble the Golgi apparatus. J Cell Biol. 2001 Mar 5;152(5):945-58. PubMed PMID: 11238451. Pubmed Central PMCID: 2198800.
33. Kraft C, Herzog F, Gieffers C, Mechtler K, Hagting A, Pines J, et al. Mitotic regulation of the human anaphase-promoting complex by phosphorylation. EMBO J. 2003 Dec 15;22(24):6598-609. PubMed PMID: 14657031. Pubmed Central PMCID: 291822.
34. Shteinberg M, Protopopov Y, Listovsky T, Brandeis M, Hershko A. Phosphorylation of the cyclosome is required for its stimulation by Fizzy/cdc20. Biochem Biophys Res Commun. 1999 Jun 24;260(1):193-8. PubMed PMID: 10381365.
35. Zachariae W, Schwab M, Nasmyth K, Seufert W. Control of cyclin ubiquitination by CDK-regulated binding of Hct1 to the anaphase promoting complex. Science. 1998 Nov 27;282(5394):1721-4. PubMed PMID: 9831566.
36. Glotzer M, Murray AW, Kirschner MW. Cyclin is degraded by the ubiquitin pathway. Nature. 1991 Jan 10;349(6305):132-8. PubMed PMID: 1846030.
37. Chang DC, Xu N, Luo KQ. Degradation of cyclin B is required for the onset of anaphase in Mammalian cells. J Biol Chem. 2003 Sep 26;278(39):37865-73. PubMed PMID: 12865421.
38. Hershko A. Mechanisms and regulation of the degradation of cyclin B. Philos Trans R Soc Lond B Biol Sci. 1999 Sep 29;354(1389):1571-5; discussion 5-6. PubMed PMID: 10582242. Pubmed Central PMCID: 1692665.
39. Fang G, Yu H, Kirschner MW. Direct binding of CDC20 protein family members activates the anaphase-promoting complex in mitosis and G1. Mol Cell. 1998 Aug;2(2):163-71. PubMed PMID: 9734353.
40. Bertoli C, Skotheim JM, de Bruin RA. Control of cell cycle transcription during G1 and S phases. Nat Rev Mol Cell Biol. 2013 Aug;14(8):518-28. PubMed PMID: 23877564. Pubmed Central PMCID: 4569015.
41. Lobrich M, Jeggo PA. The impact of a negligent G2/M checkpoint on genomic instability and cancer induction. Nat Rev Cancer. 2007 Nov;7(11):861-9. PubMed PMID: 17943134.

42. Jackson SP, Bartek J. The DNA-damage response in human biology and disease. Nature. 2009 Oct 22;461(7267):1071-8. PubMed PMID: 19847258. Pubmed Central PMCID: 2906700.
43. Collin P, Nashchekina O, Walker R, Pines J. The spindle assembly checkpoint works like a rheostat rather than a toggle switch. Nat Cell Biol. 2013 Nov;15(11):1378-85. PubMed PMID: 24096242. Pubmed Central PMCID: 3836401.
44. Sacristan C, Kops GJ. Joined at the hip: kinetochores, microtubules, and spindle assembly checkpoint signaling. Trends Cell Biol. 2015 Jan;25(1):21-8. PubMed PMID: 25220181.
45. Lampson MA, Cheeseman IM. Sensing centromere tension: Aurora B and the regulation of kinetochore function. Trends Cell Biol. 2011 Mar;21(3):133-40. PubMed PMID: 21106376. Pubmed Central PMCID: 3049846.
46. Li Y, Gorbea C, Mahaffey D, Rechsteiner M, Benezra R. MAD2 associates with the cyclosome/anaphase-promoting complex and inhibits its activity. Proc Natl Acad Sci U S A. 1997 Nov 11;94(23):12431-6. PubMed PMID: 9356466. Pubmed Central PMCID: 24983.
47. Fang G, Yu H, Kirschner MW. The checkpoint protein MAD2 and the mitotic regulator CDC20 form a ternary complex with the anaphase-promoting complex to control anaphase initiation. Genes & development. 1998 Jun 15;12(12):1871-83. PubMed PMID: 9637688. Pubmed Central PMCID: 316912.
48. Fang G. Checkpoint protein BubR1 acts synergistically with Mad2 to inhibit anaphase-promoting complex. Mol Biol Cell. 2002 Mar;13(3):755-66. PubMed PMID: 11907259. Pubmed Central PMCID: 99596.
49. Izawa D, Pines J. The mitotic checkpoint complex binds a second CDC20 to inhibit active APC/C. Nature. 2015 Jan 29;517(7536):631-4. PubMed PMID: 25383541. Pubmed Central PMCID: 4312099.
50. Teixeira LK, Reed SI. Ubiquitin ligases and cell cycle control. Annu Rev Biochem. 2013;82:387-414. PubMed PMID: 23495935.
51. Bochis OV, Fetica B, Vlad C, Achimas-Cadariu P, Irimie A. The Importance of Ubiquitin E3 Ligases, SCF and APC/C, in Human Cancers. Clujul Med. 2015;88(1):9-14. PubMed PMID: 26528041. Pubmed Central PMCID: 4508606.
52. Hershko A, Ciechanover A. The ubiquitin system. Annu Rev Biochem. 1998;67:425-79. PubMed PMID: 9759494.
53. Hochegger H, Takeda S, Hunt T. Cyclin-dependent kinases and cell-cycle transitions: does one fit all? Nat Rev Mol Cell Biol. 2008 Nov;9(11):910-6. PubMed PMID: 18813291.
54. Bhoj VG, Chen ZJ. Ubiquitylation in innate and adaptive immunity. Nature. 2009 Mar 26;458(7237):430-7. PubMed PMID: 19325622.
55. Nalepa G, Wade Harper J. Therapeutic anti-cancer targets upstream of the proteasome. Cancer Treat Rev. 2003 May;29 Suppl 1:49-57. PubMed PMID: 12738243.
56. Bashir T, Dorrello NV, Amador V, Guardavaccaro D, Pagano M. Control of the SCF(Skp2-Cks1) ubiquitin ligase by the APC/C(Cdh1) ubiquitin ligase. Nature. 2004 Mar 11;428(6979):190-3. PubMed PMID: 15014502.
57. Nakayama KI, Nakayama K. Ubiquitin ligases: cell-cycle control and cancer. Nat Rev Cancer. 2006 May;6(5):369-81. PubMed PMID: 16633365.
58. Frescas D, Pagano M. Deregulated proteolysis by the F-box proteins SKP2 and beta-TrCP: tipping the scales of cancer. Nat Rev Cancer. 2008 Jun;8(6):438-49. PubMed PMID: 18500245. Pubmed Central PMCID: 2711846.
59. Margottin-Goguet F, Hsu JY, Loktev A, Hsieh HM, Reimann JD, Jackson PK. Prophase destruction of Emi1 by the SCF(betaTrCP/Slimb) ubiquitin ligase activates the anaphase promoting complex to allow progression beyond prometaphase. Dev Cell. 2003 Jun;4(6):813-26. PubMed PMID: 12791267.
60. Zhou Z, He M, Shah AA, Wan Y. Insights into APC/C: from cellular function to diseases and therapeutics. Cell Div. 2016;11:9. PubMed PMID: 27418942. Pubmed Central PMCID: 4944252.

61. Sullivan M, Morgan DO. Finishing mitosis, one step at a time. Nat Rev Mol Cell Biol. 2007 Nov;8(11):894-903. PubMed PMID: 17912263.
62. Pfleger CM, Kirschner MW. The KEN box: an APC recognition signal distinct from the D box targeted by Cdh1. Genes Dev. 2000 Mar 15;14(6):655-65. PubMed PMID: 10733526. Pubmed Central PMCID: 316466.
63. Izawa D. How APC/C–Cdc20 changes its substrate specificity in mitosis. Nature Cell Biology. 2011;13:223-33.
64. Kabeche L, Compton DA. Cyclin A regulates kinetochore microtubules to promote faithful chromosome segregation. Nature. 2013 Oct 3;502(7469):110-3. PubMed PMID: 24013174. Pubmed Central PMCID: 3791168.
65. Boekhout M, Wolthuis R. Nek2A destruction marks APC/C activation at the prophase-to-prometaphase transition by spindle-checkpoint-restricted Cdc20. J Cell Sci. 2015 Apr 15;128(8):1639-53. PubMed PMID: 25673878.
66. Furuno N, den Elzen N, Pines J. Human cyclin A is required for mitosis until mid prophase. J Cell Biol. 1999 Oct 18;147(2):295-306. PubMed PMID: 10525536. Pubmed Central PMCID: 2174228.
67. Gong D, Pomerening JR, Myers JW, Gustavsson C, Jones JT, Hahn AT, et al. Cyclin A2 regulates nuclear-envelope breakdown and the nuclear accumulation of cyclin B1. Curr Biol. 2007 Jan 9;17(1):85-91. PubMed PMID: 17208191. Pubmed Central PMCID: 1830184.
68. Visintin R, Craig K, Hwang ES, Prinz S, Tyers M, Amon A. The phosphatase Cdc14 triggers mitotic exit by reversal of Cdk-dependent phosphorylation. Mol Cell. 1998 Dec;2(6):709-18. PubMed PMID: 9885559.
69. Chang L, Zhang Z, Yang J, McLaughlin SH, Barford D. Molecular architecture and mechanism of the anaphase-promoting complex. Nature. 2014 Sep 18;513(7518):388-93. PubMed PMID: 25043029.
70. Huang JY, Raff JW. The dynamic localisation of the Drosophila APC/C: evidence for the existence of multiple complexes that perform distinct functions and are differentially localised. J Cell Sci. 2002 Jul 15;115(Pt 14):2847-56. PubMed PMID: 12082146.
71. Zieba A, Grannas K, Soderberg O, Gullberg M, Nilsson M, Landegren U. Molecular tools for companion diagnostics. N Biotechnol. 2012 Sep 15;29(6):634-40. PubMed PMID: 22634023.
72. Soderberg O, Gullberg M, Jarvius M, Ridderstrale K, Leuchowius KJ, Jarvius J, et al. Direct observation of individual endogenous protein complexes in situ by proximity ligation. Nat Methods. 2006 Dec;3(12):995-1000. PubMed PMID: 17072308.
73. Gullberg M, Fredriksson S, Taussig M, Jarvius J, Gustafsdottir S, Landegren U. A sense of closeness: protein detection by proximity ligation. Curr Opin Biotechnol. 2003 Feb;14(1):82-6. PubMed PMID: 12566006.
74. Thymiakou E, Episkopou V. Detection of signaling effector-complexes downstream of bmp4 using PLA, a proximity ligation assay. J Vis Exp. 2011 (49). PubMed PMID: 21403637. Pubmed Central PMCID: 3197320.
75. Ke R, Nong RY, Fredriksson S, Landegren U, Nilsson M. Improving precision of proximity ligation assay by amplified single molecule detection. PLoS One. 2013;8(7):e69813. PubMed PMID: 23874999. Pubmed Central PMCID: 3713053.
76. Zeng X, Sigoillot F, Gaur S, Choi S, Pfaff KL, Oh DC, et al. Pharmacologic inhibition of the anaphase-promoting complex induces a spindle checkpoint-dependent mitotic arrest in the absence of spindle damage. Cancer Cell. 2010 Oct 19;18(4):382-95. PubMed PMID: 20951947. Pubmed Central PMCID: PMC2957475.
77. Greenwood C, Ruff D, Kirvell S, Johnson G, Dhillon HS, Bustin SA. Proximity assays for sensitive quantification of proteins. Biomol Detect Quantif. 2015 Jun;4:10-6. PubMed PMID: 27077033. Pubmed Central PMCID: PMC4822221.
78. Sivakumar S, Gorbsky GJ. Spatiotemporal regulation of the anaphase-promoting complex in mitosis. Nat Rev Mol Cell Biol. 2015 Feb;16(2):82-94. PubMed PMID: 25604195. Pubmed Central PMCID: PMC4386896.

84. Musacchio A. The Molecular Biology of Spindle Assemble Checkpoint Signalling Dynamics. Current Biology Review. 2015; R1002-1018.

85. Heald R, Khodjakov A. Thirty years of search and capture: The complex simplicity mitotic spindle assembly. JCB Review. 2015;6: 1003-1011.

86. Ji Z, Gao H, Yu H. Kinetochore attachment sensed by competitive Mps1 and microtubule binding to Ndc80C. SCIENCE report. 2015;384: 1260-1263.